Electronic Supplementary Material (ESI) for Green Chemistry.
This journal is © The Royal Society of Chemistry 2022

Pd-functionalized polydopamine-coated polyurethane foam: a readily prepared and highly reusable structured catalyst for selective alkyne semi-hydrogenation and Suzuki coupling under air

Han Peng,[a] Xiong Zhang,[b] Vasiliki Papaefthimiou,[b] Cuong Pham-Huu*[b] and Vincent Ritleng*[a]

[a] Université de Strasbourg, Ecole européenne de Chimie, Polymères et Matériaux, CNRS, LIMA, UMR 7042, 25 rue Becquerel, 67087 Strasbourg, France. vritleng@unistra.fr

[b] Institute of Chemistry and Processes for Energy, Environment and Health (ICPEES), ECPM, UMR 7515 CNRS-University of Strasbourg, 25 rue Becquerel, 67087 Strasbourg Cedex 02, France. cuong.pham-huu@unistra.fr

Contents

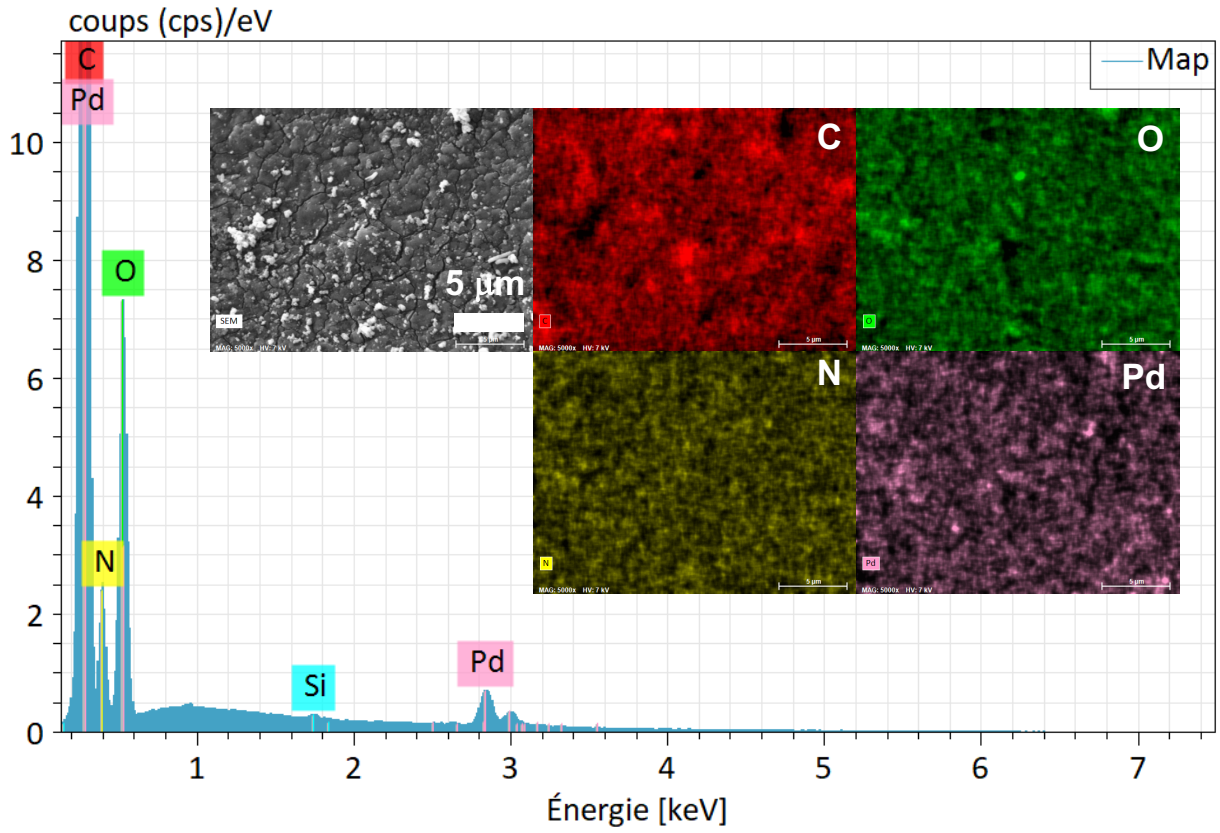

Figure S1. SEM-EDX spectrum and elemental mapping of as-synthesized Pd@PDA@PUF.

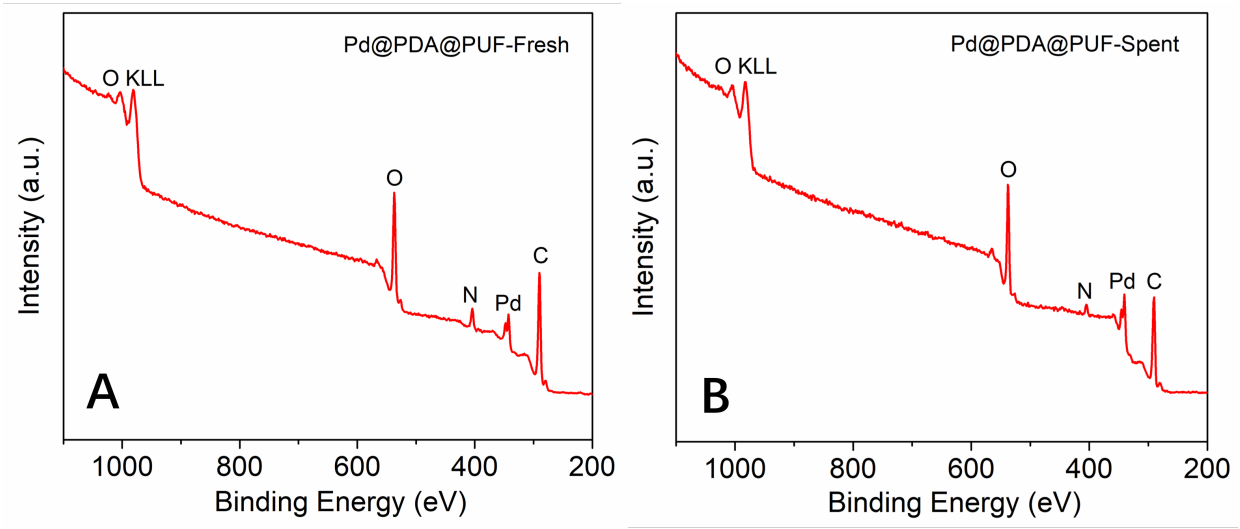

Figure S2. XPS survey spectra of Pd@PDA@PUF: (A) as-synthesized, (B) spent (after 15 cycling tests).

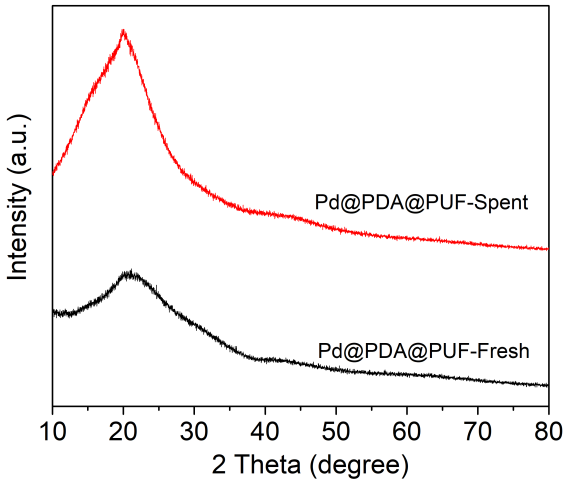

Figure S3. XRD profiles of Pd@PDA@PUF: black curve, as-synthesized; red curve, spent (after 15 cycling tests).

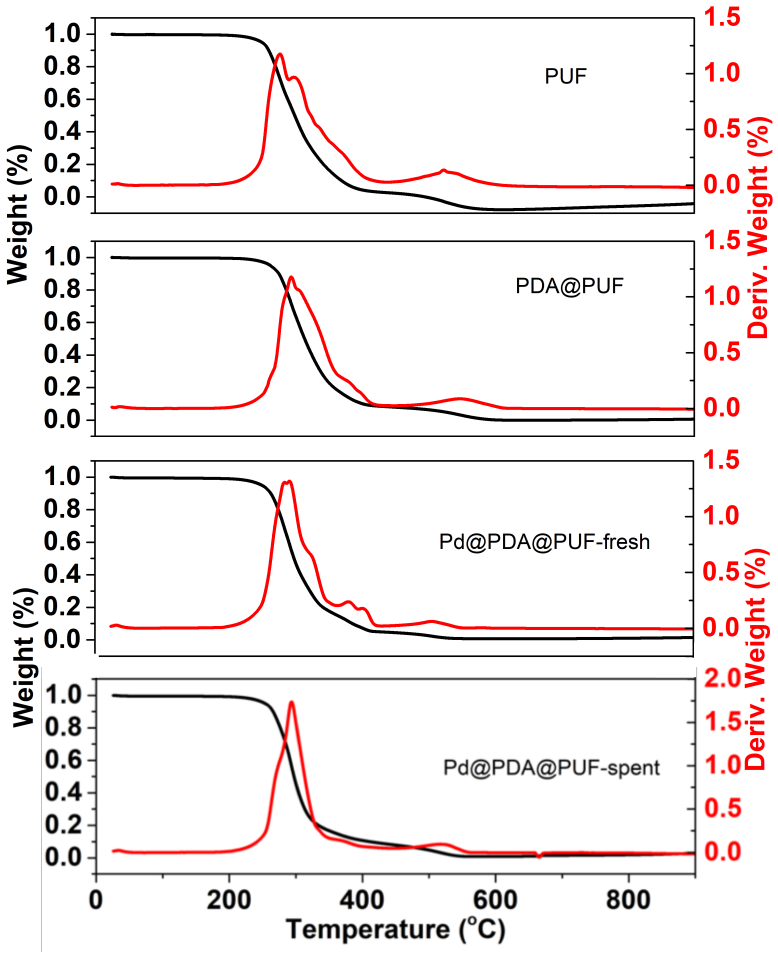

Figure S4. TGA curves of PUF, PDA@PUF, as-synthesized Pd@PDA@PUF and spent Pd@PDA@PUF (after 15 cycling tests).

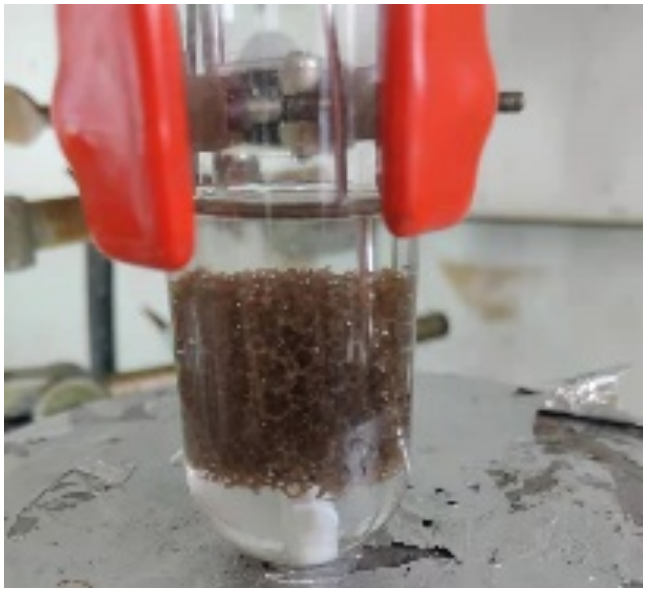

Figure S5. Standard setup for all semi-hydrogenation experiments.

Optimization studies for the semi-hydrogenation of phenylacetylene (PA) to styrene (ST) with Pd@PDA@PUF in EtOH at RT

All successive experiments were carried out with the same Pd@PDA@PUF foam of *ca.* 8 cm^3 whose mass was adjusted in function of its Pd content to have a Pd loading of 7 μmol. The two first trials, run with a Pd loading of 0.46 mol% and a H_2 flow of 13 mL/min, displayed similar reaction kinetics, with 98% conversion of PA and 97% selectivity to ST after 3.3 h for the 1st run (TON = 213, TOF = 65 h^{-1}), and 93% conversion and 90% ST selectivity after 3 h in the 2nd run (TON = 202, TOF = 67 h^{-1}) (Table S1, entries A and B). Once all alkyne had been consumed, the selectivity began to drop down as over-hydrogenation occurred (Fig. S6A and S6B). In view of these encouraging results, notably the little acceleration of the reaction kinetics between the two runs, we performed a third run under the same conditions. As can be seen in Figure S6C, we again observed a very selective conversion of PA to ST without any appreciable competition of further hydrogenation of the latter to give ethylbenzene (EB) until all PA had been consumed. Thus, 97% conversion was reached in 3 h with a ST selectivity of 88% (TON = 211, TOF = 70 h^{-1}) (Table S1, entry C). In the 4th run, the rate of H_2 flow was decreased from 13 to 2 mL/min in order to map out its influence on the catalytic performance. No positive effect was observed on the hydrogenation selectivity, as only 94% ST selectivity at 81% PA conversion was observed after 2 h reaction and as it dropped similarly one all PA was consumed (Figure S6D and Table S1, entry D). We thus maintained the H_2 flow rate to 13 mL/min for the next two experiments, but increased the reactant's concentration to 3 and 6 mmol, conversely decreasing the catalyst loading from 0.46 mol% to 0.23 mol% in the 5th run (Figure S6E) and to 0.11 mol% in the 6th run (Figure S6F). Remarkably, the Pd@PDA@PUF catalyst maintained a very high chemoselectivity with higher kinetics in the 5th run, achieving as high as 91% conversion with 95% selectivity to ST after 2 h (TON = 396; TOF = 197 h^{-1}) (Table S1, entry E). Again, ST hydrogenation to EB occurred appreciably only after full consumption of PA. When the substrate loading was doubled again to 6 mmol, the selectivity and the turnover frequency gratifyingly maintained to the same level, with 98% PA conversion with 94% selectivity after 4.25 h, thus giving a TON of 891 and a TOF of 210 h^{-1} (Table S1, entry F). The latter conditions were chosen as the standard conditions.

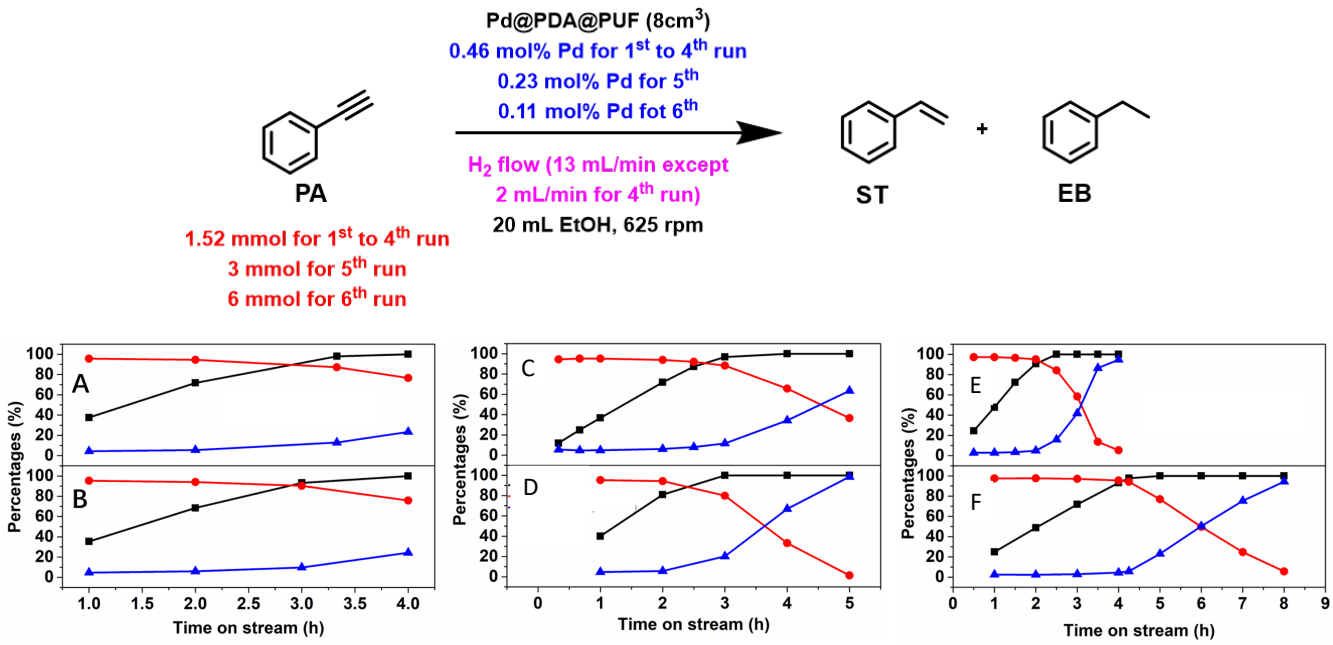

Figure S6. Kinetic monitoring of the optimization tests of PA semi-hydrogenation with Pd@PDA@PUF (*ca.* 8 cm^3, Pd content $7.00.10^{-3}$ mmol) in EtOH (20 mL) at RT under 625 rpm. **A, B, C**: PA (1.52 mmol), H_2 (13 mL/min); **D:** PA (1.52 mmol), H_2 (2 mL/min); **E:** PA (3 mmol), H_2 (13 mL/min); **F:** PA (6 mmol), H_2 (13 mL/min). Black curves: PA conversion. Red curves: selectivity to ST. Blue curves: selectivity to ethylbenzene (EB).

Table S1. Results of optimization tests of PA semi-hydrogenation to ST.

Entry	Cat. loading (Pd mol%)	H_2 flow speed	Time (h)	Conv. (%)[a]	Select. (%)[a]	TON[b]	TOF (h^{-1})
A	0.46	13	3.3	98	97	207	63
B	0.46	13	3	93	90	182	61
C	0.46	13	3	97	88	186	62
D	0.46	2	2	81	94	166	83
E	0.23	13	2	91	95	376	188
F	0.12	13	4.25	98	95	776	183

[a] PA conversion and ST selectivity were determined by GC analysis. [b] Turnover number expressed as mol of PA converted to ST *vs*. the catalytic loading.

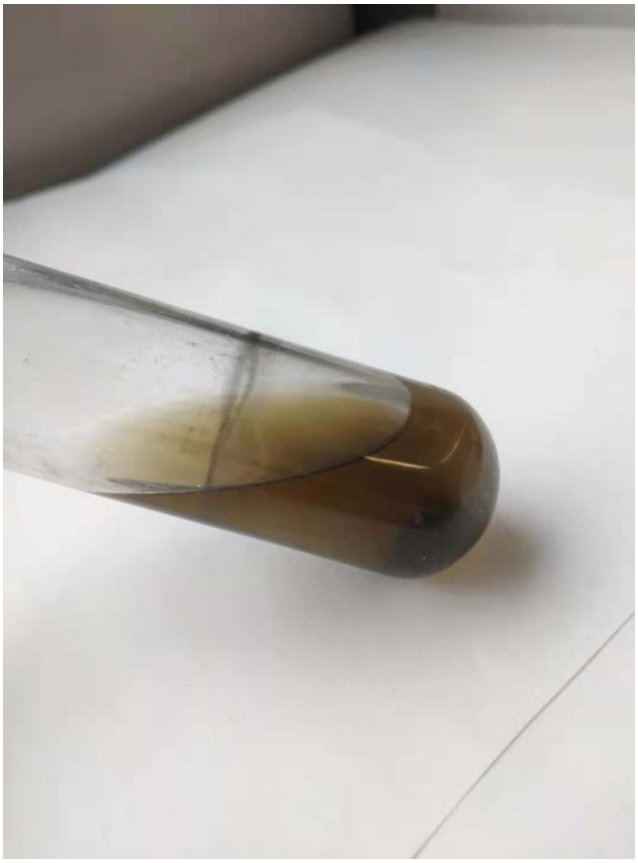

Figure S7. Photo of the reaction medium after the hydrogenation of phenylacetylene with $[Pd(NH_3)_4Cl_2]\cdot H_2O$ (0.23 mol%).

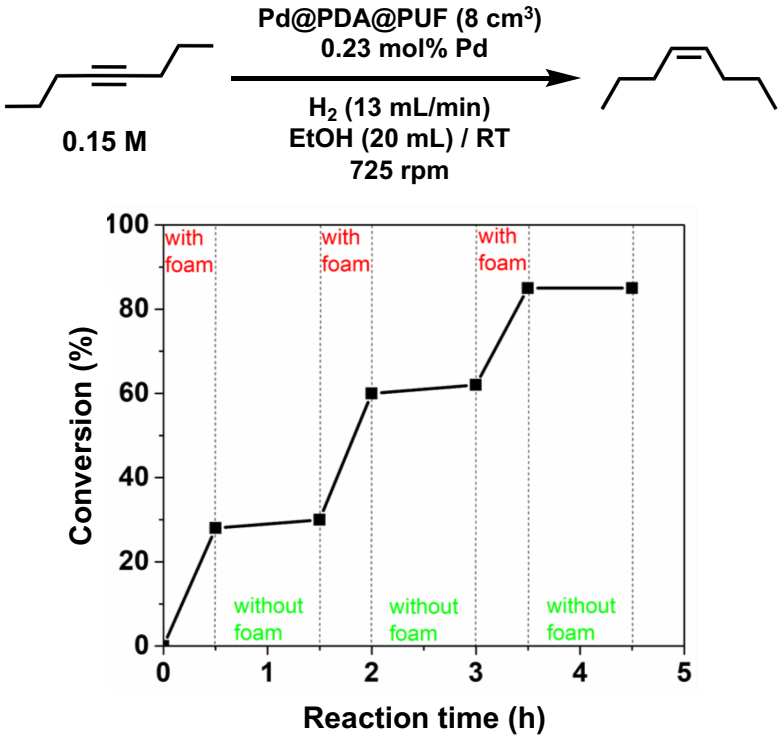

Figure S8. Stop-and-go experiment on 4-octyne' semi-hydrogenation with Pd@PDA@PUF. Reaction conditions: 4-octyne (3 mmol), Pd@PUF@PDA (8 cm^3, Pd: 0.23 mol%), EtOH (20 mL), H_2 flow rate (13 mL/min), room temperature, 625 rpm.

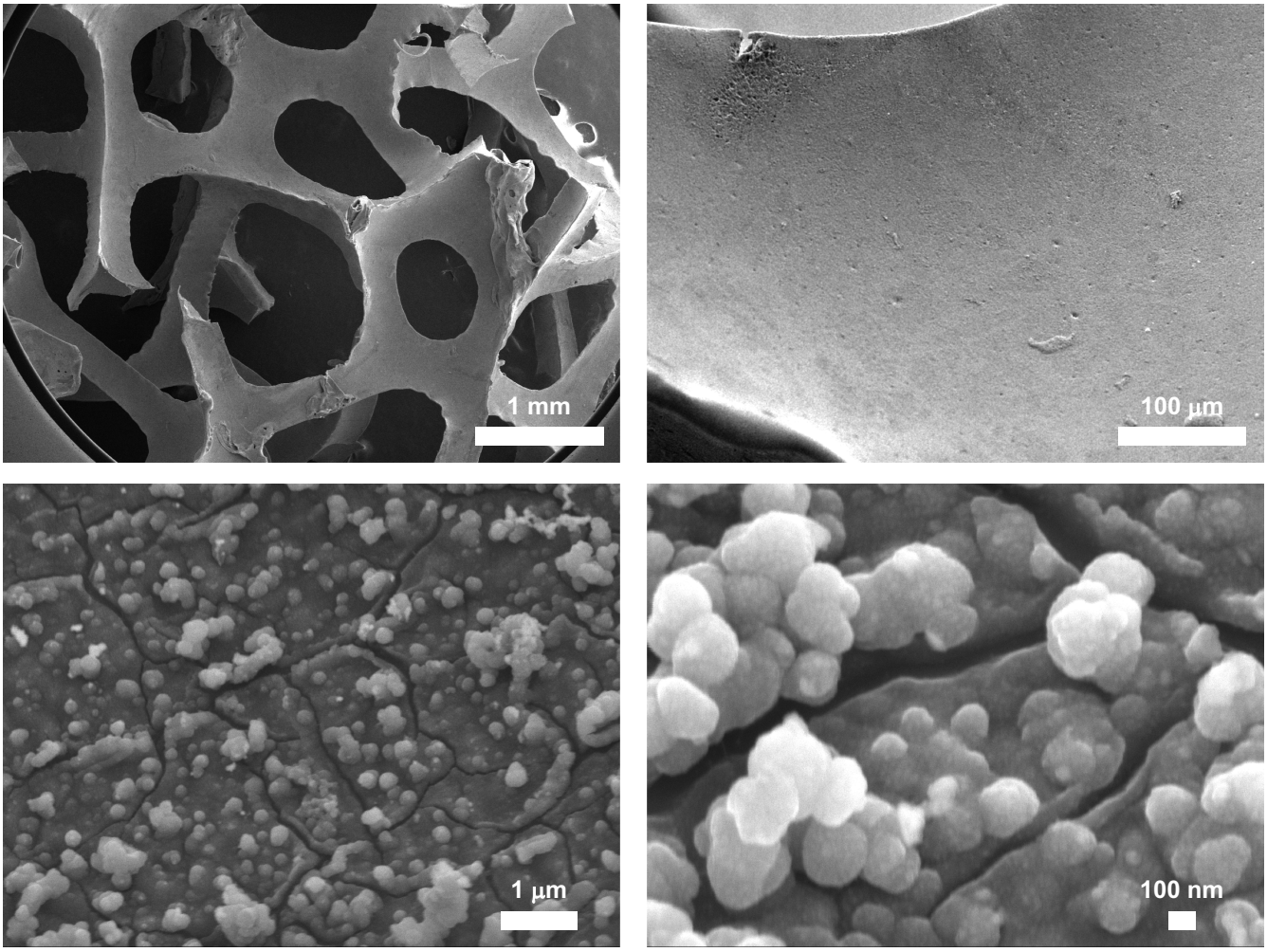

Figure S9. HR-SEM images with different magnifications of spent Pd@PDA@PUF (after 15 cycling tests).

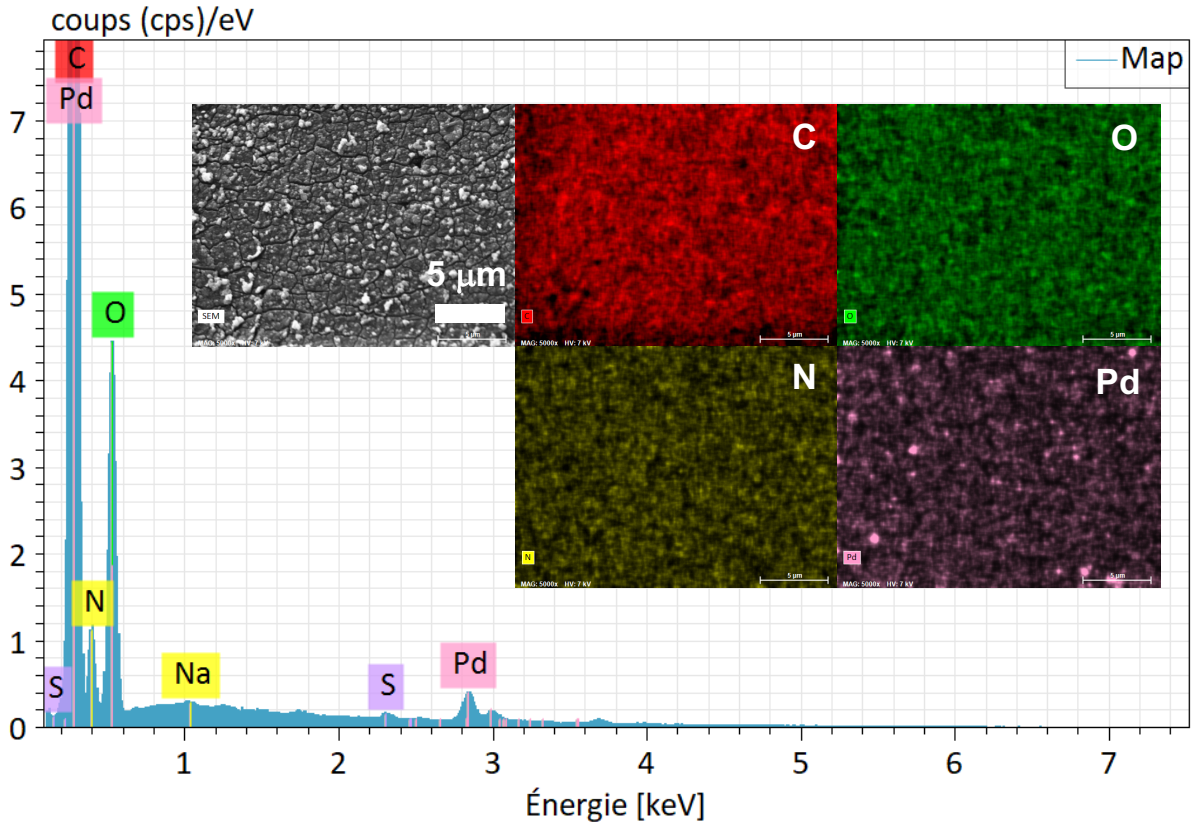

Figure S10. SEM-EDX spectrum and elemental maps of spent Pd@PDA@PUF (after 15 cycling tests).

$$\text{Conversion} = \frac{\frac{a}{4}+\frac{c}{2}+\frac{d}{4}}{\frac{b}{4}+\frac{a}{4}+\frac{c}{2}+\frac{d}{4}} \times 100\%$$

$$\text{Selectivity ((}Z\text{)-1,2-diphenylethene)} = \frac{\frac{c}{2}}{\frac{a}{4}+\frac{c}{2}+\frac{d}{4}} \times 100\%$$

1 h

$$\text{Selectivity ((}E\text{)-1,2-diphenylethene)} = \frac{\frac{a}{4}}{\frac{a}{4}+\frac{c}{2}+\frac{d}{4}} \times 100\%$$

$$\text{Selectivity (1,2-diphenylethane)} = \frac{\frac{d}{4}}{\frac{a}{4}+\frac{c}{2}+\frac{d}{4}} \times 100\%$$

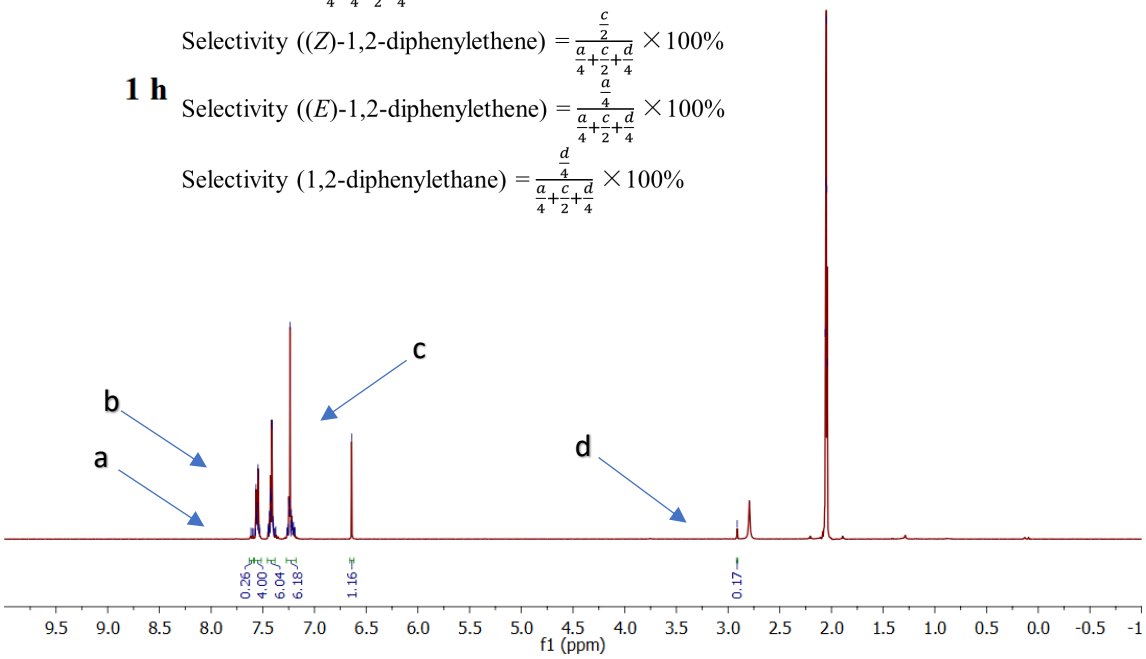

2 h

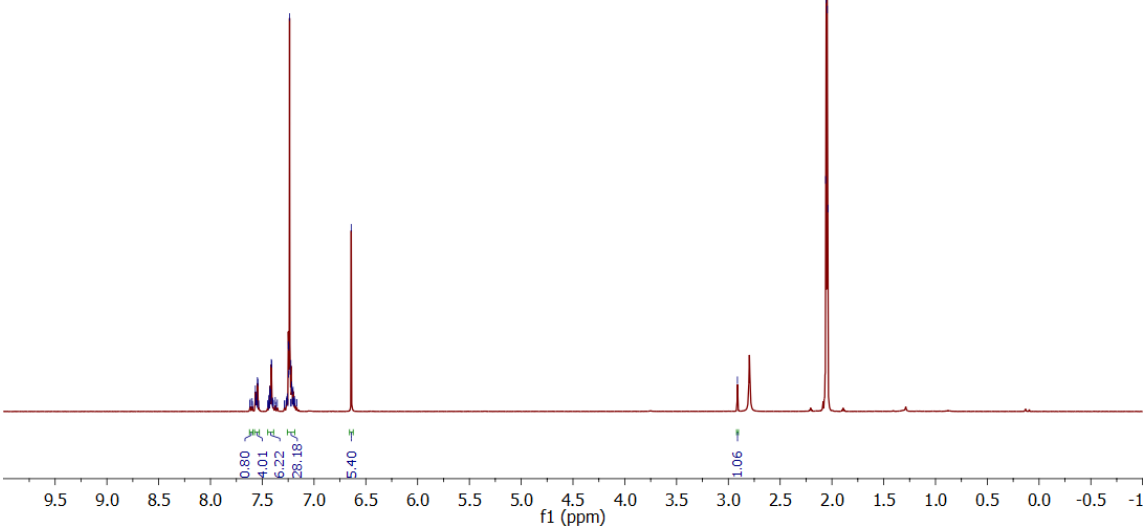

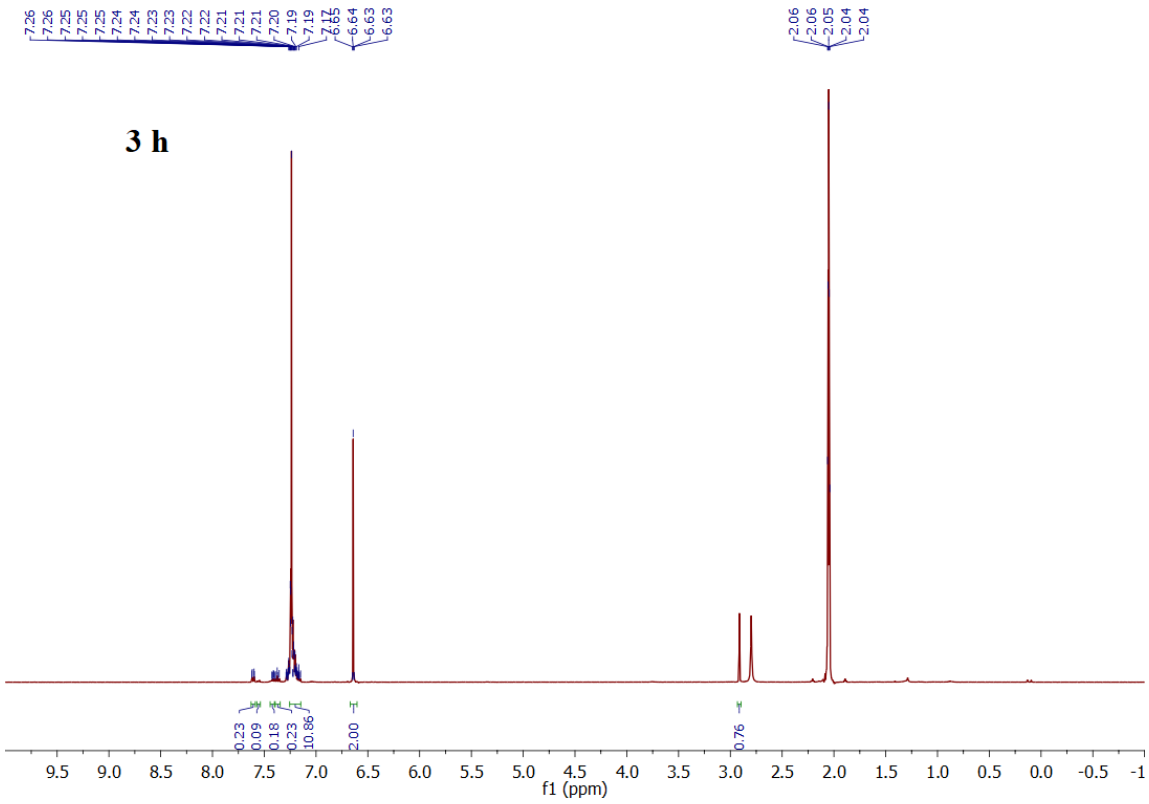
3 h
f1 (ppm)

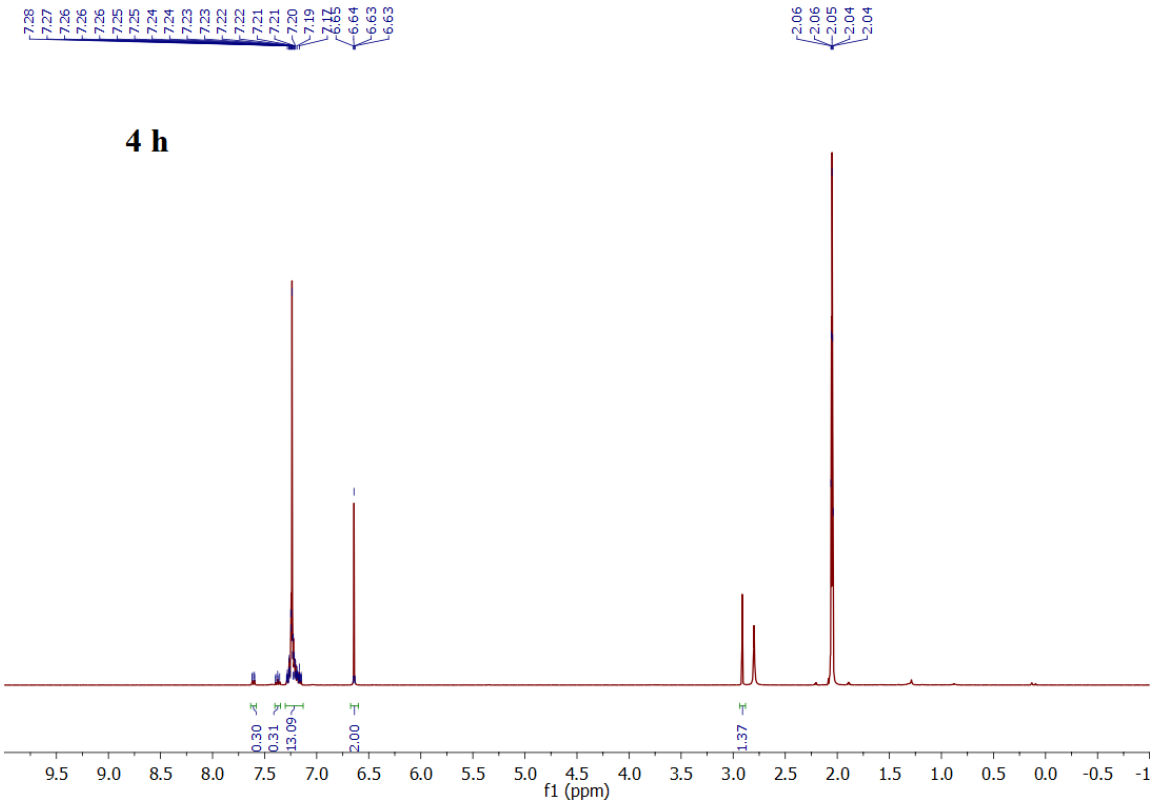
4 h
f1 (ppm)

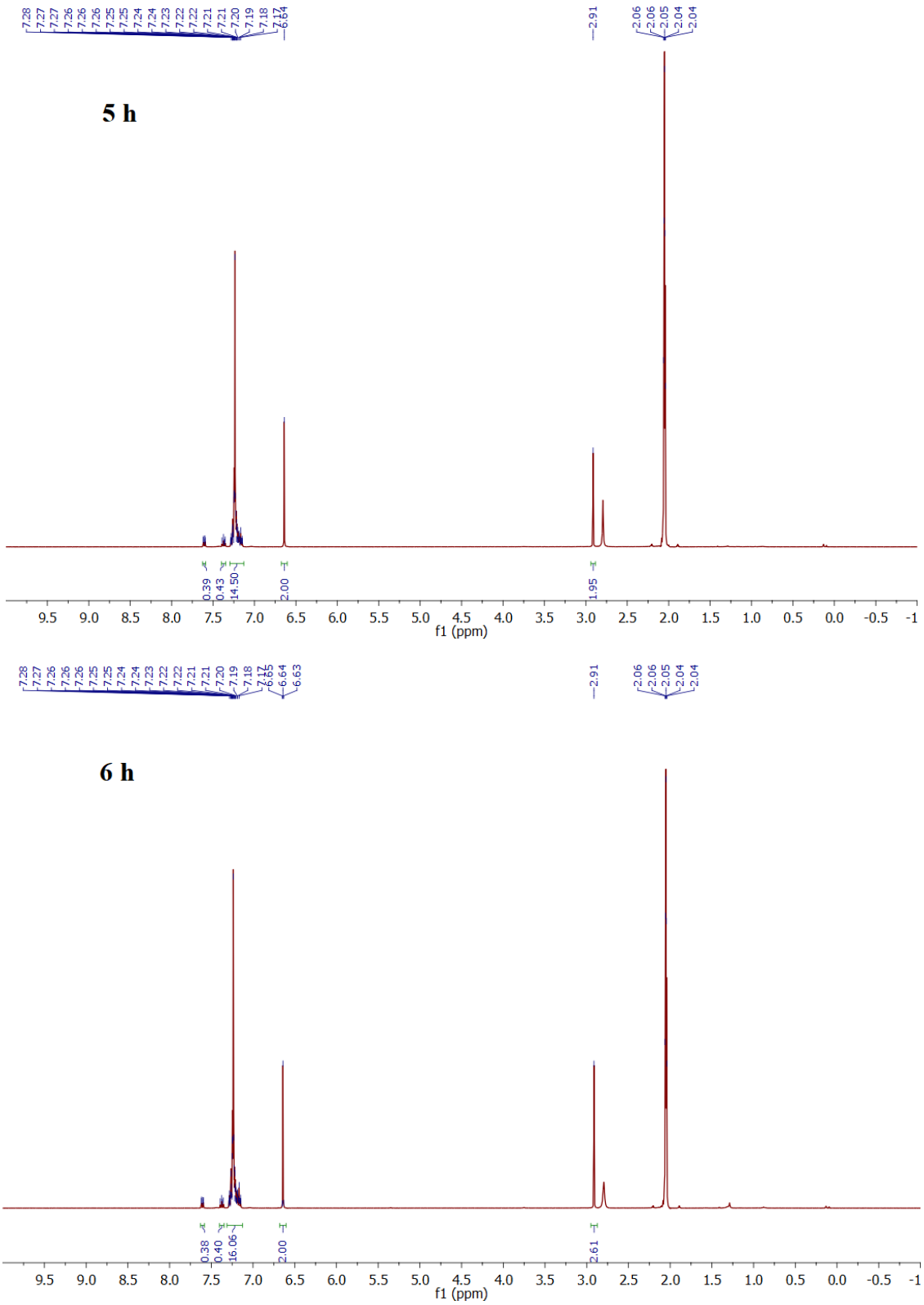

Figure S11. ^{1}H NMR ($(CD_3)_2CO$, 400.13 MHz) spectra of the reaction mixture of the semi-hydrogenation of 1,2-diphenylethyne after 1, 2, 3, 4, 5 and 6 h reaction.

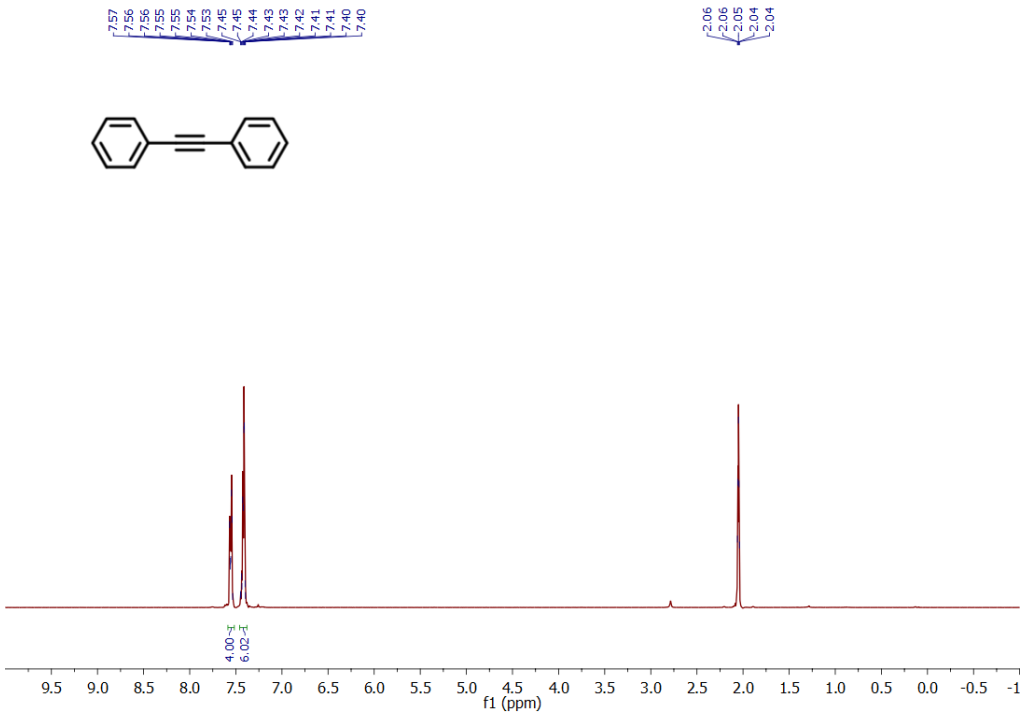

Figure S12. ^{1}H NMR ($(CD_3)_2CO$, 400.13 MHz)) spectrum of 1,2-diphenylethyne.

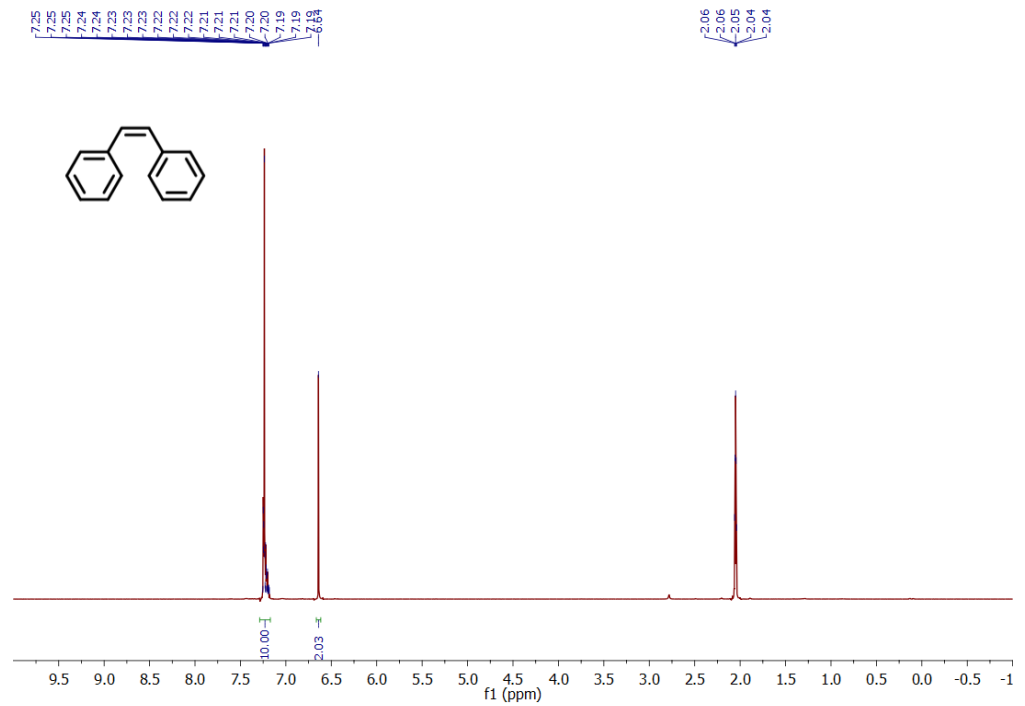

Figure S13. ^{1}H NMR ($(CD_3)_2CO$, 400.13 MHz)) spectrum of (*Z*)-1,2-diphenylethene.

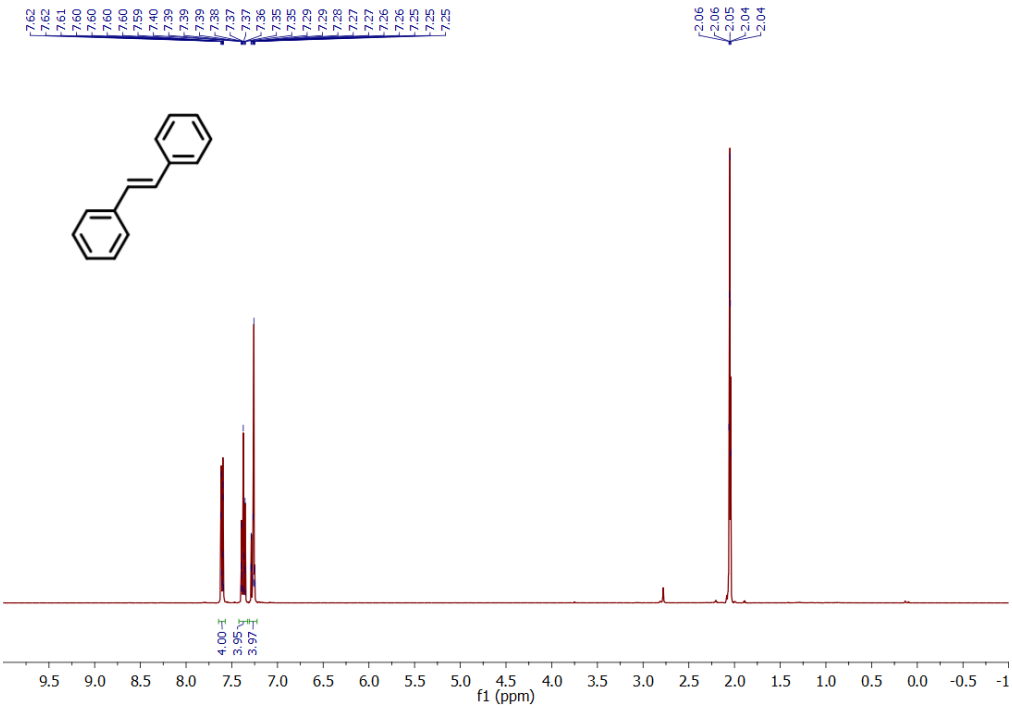

Figure S14. ^{1}H NMR ($(CD_3)_2CO$, 400.13 MHz)) spectrum of (*E*)-1,2-diphenylethene.

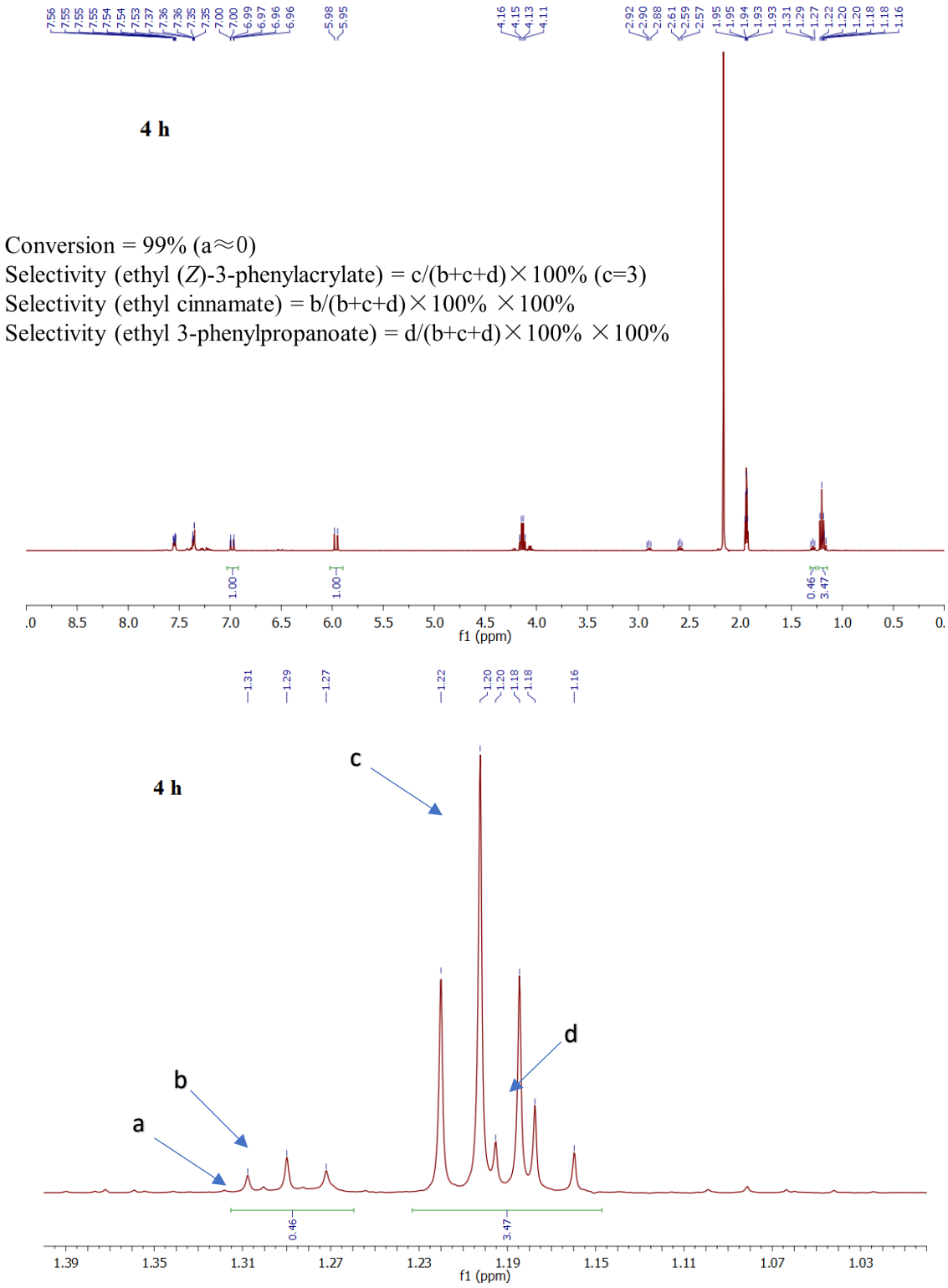

Figure S15. ^{1}H NMR (CD_3CN, 400.13 MHz) spectrum of the reaction mixture of the semi-hydrogenation of ethyl 3-phenylpropiolate after 4 h reaction.

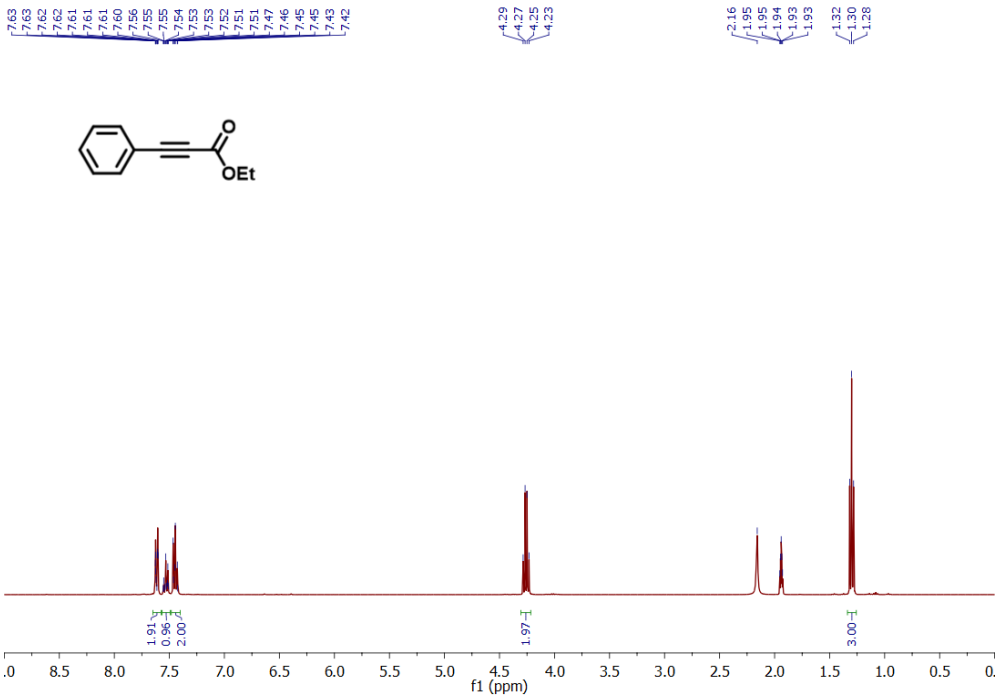

Figure S16. ^{1}H-NMR (CD_3CN, 400.13 MHz) spectrum of ethyl 3-phenylpropiolate.

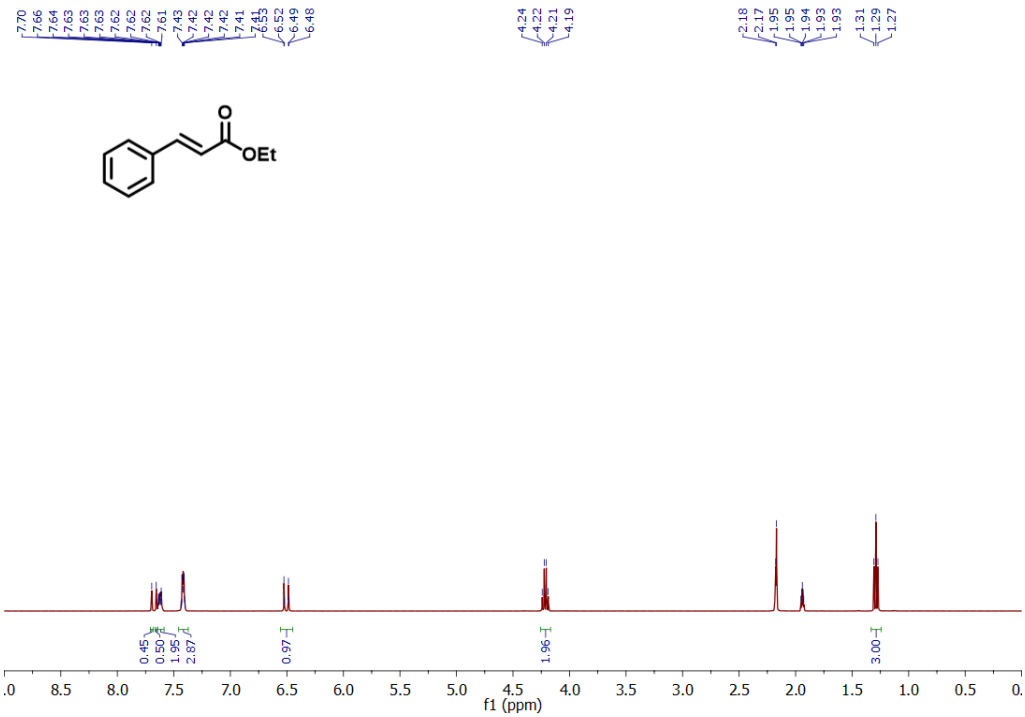

Figure S17. ^{1}H NMR (CD_3CN, 400.13 MHz) spectrum of ethyl cinnamate.

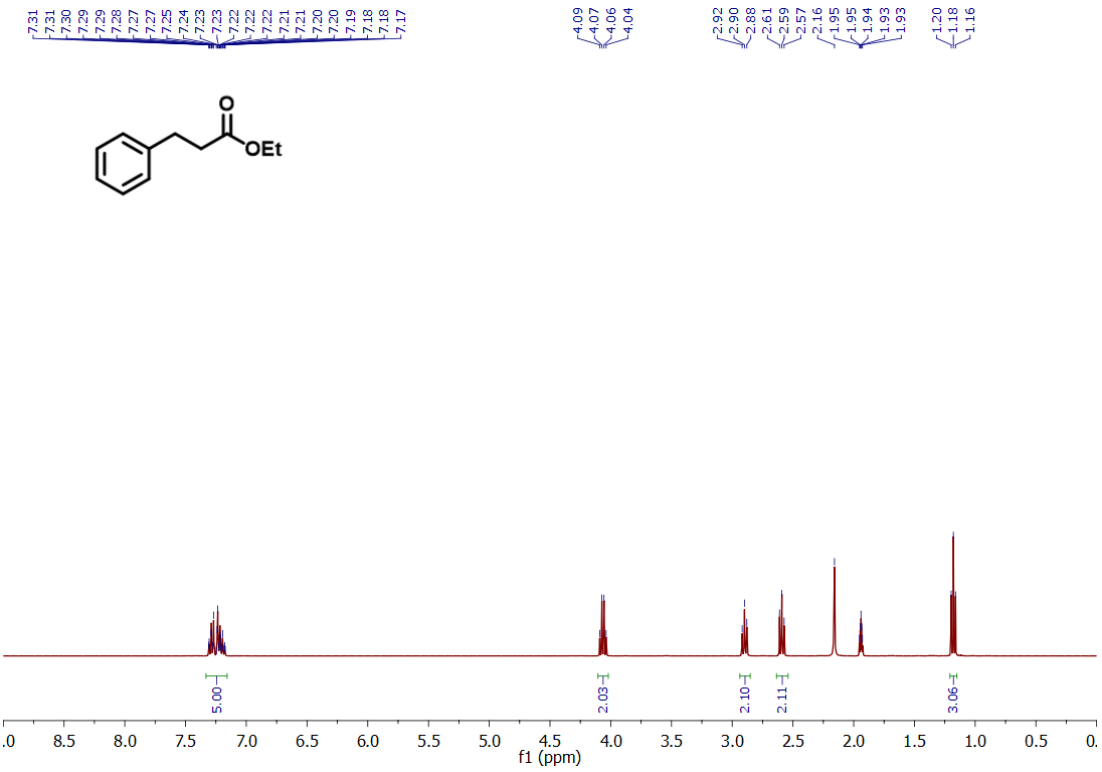

Figure S18. ^{1}H NMR (CD_3CN, 400.13 MHz) spectrum of ethyl 3-phenylpropanoate.

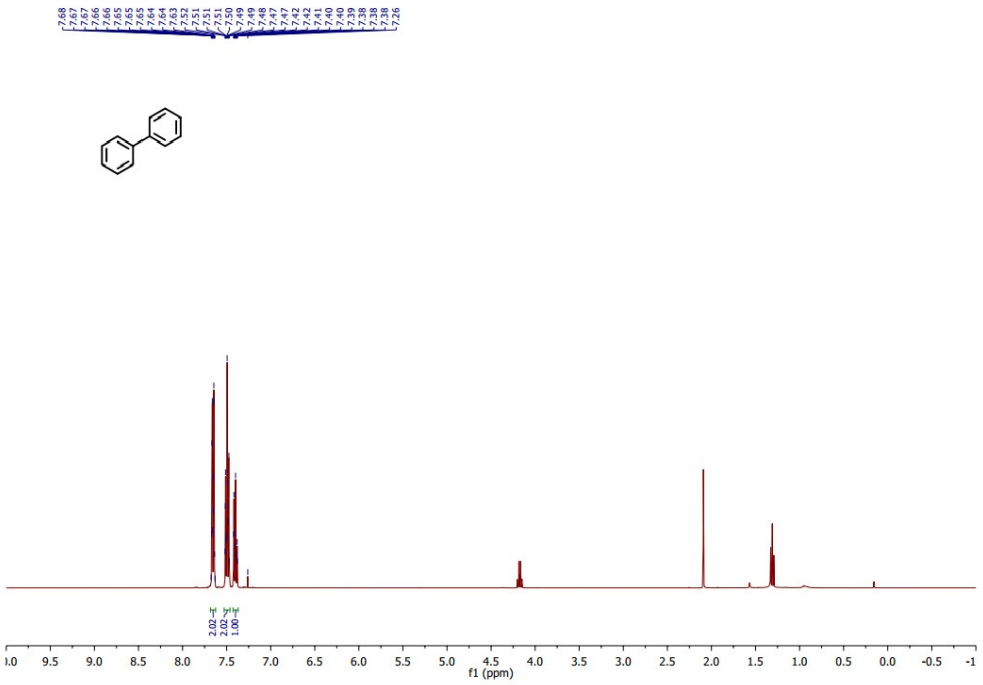

Figure S19. ^{1}H NMR ($CDCl_3$) spectrum of biphenyl.

^{1}H NMR ($CDCl_3$, 400.13 MHz): δ 7.68–7.62 (m, 4H), 7.53–7.46 (m, 4H), 7.43 – 7.37 (m, 2H).

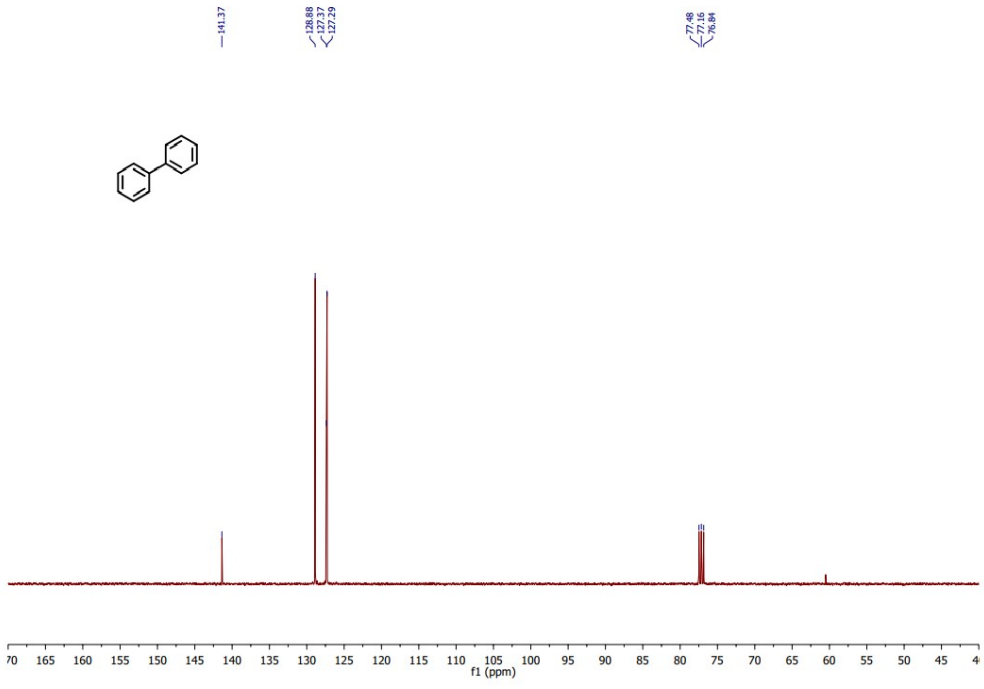

Figure S20. ^{13}C NMR ($CDCl_3$) spectrum of biphenyl.

$^{13}C\{^{1}H\}$ NMR ($CDCl_3$, 100.61 MHz): δ 141.4, 128.9, 127.4.

^{1}H and ^{13}C NMR data in agreement with the literature.[1]

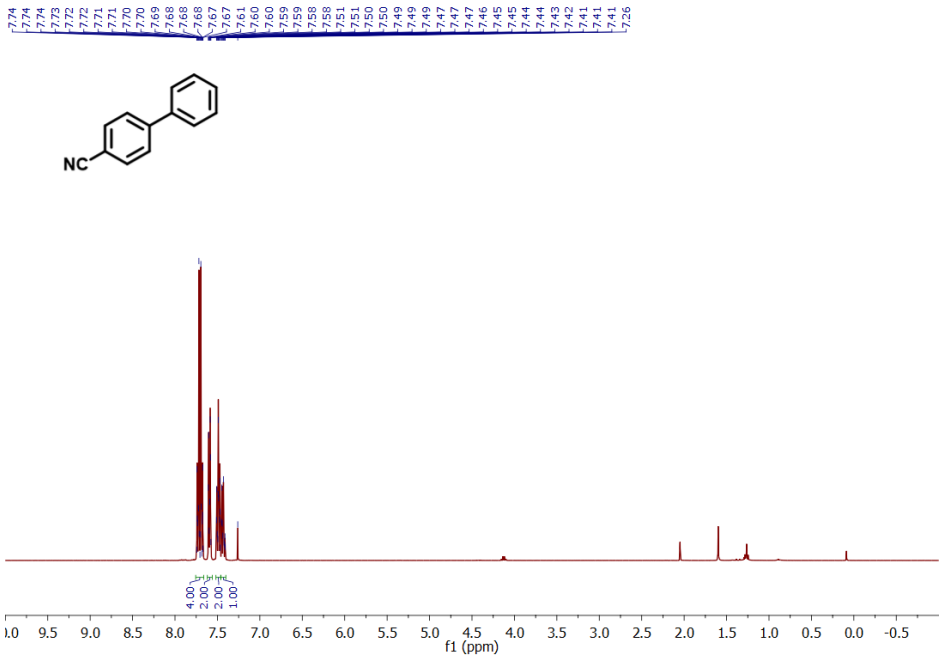

Figure S21. ^{1}H NMR ($CDCl_3$) spectrum of 4-cyanobiphenyl.

^{1}H NMR ($CDCl_3$, 400.13 MHz): δ 7.76–7.66 (m, 4H), 7.62–7.56 (m, 2H), 7.49 (tt, J = 6.5, 1.1 Hz, 2H), 7.46–7.40 (m, 1H).

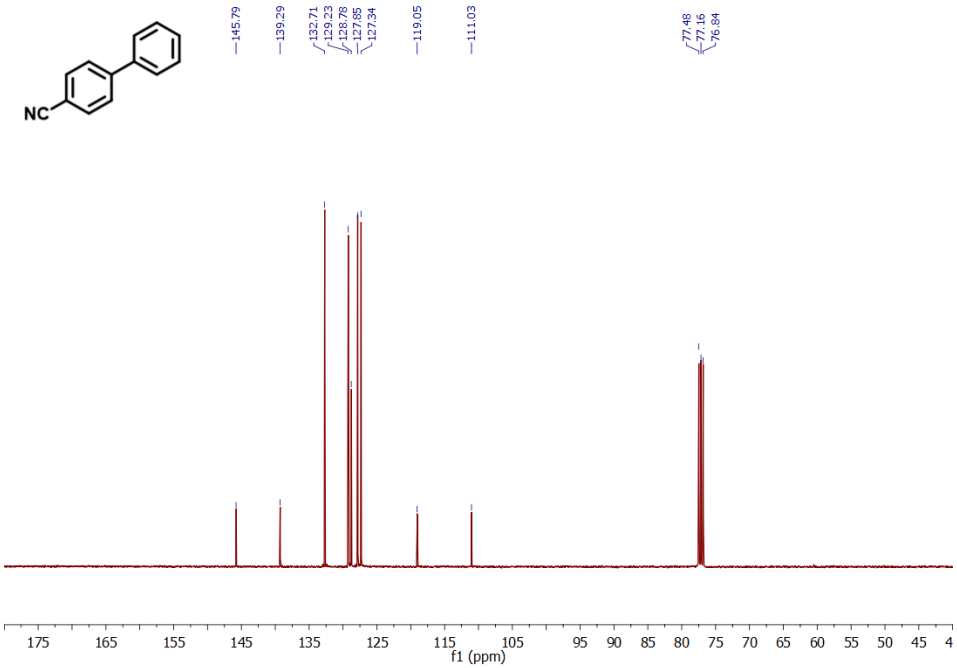

Figure S22. ^{13}C NMR ($CDCl_3$) spectrum of 4-cyanobiphenyl.

^{13}C{^{1}H} NMR ($CDCl_3$, 100.61 MHz): δ 145.8, 139.3, 132.7, 129.2, 128.8, 127.9, 127.3, 119.1, 111.0.

^{1}H and ^{13}C NMR data in agreement with the literature.[2,3]

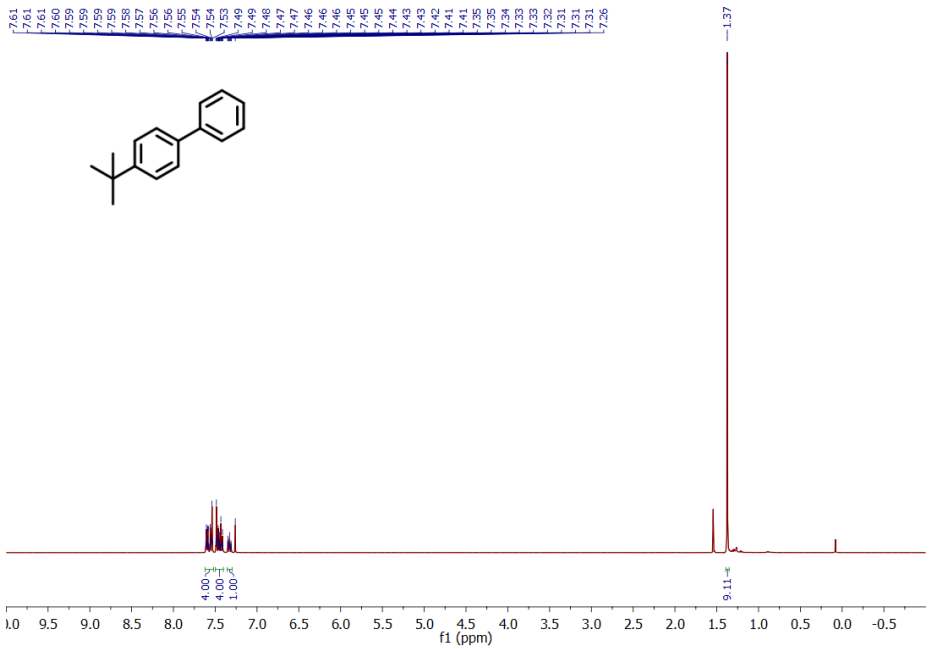

Figure S23. ^{1}H NMR ($CDCl_3$) spectrum of 4-*tert*-butylbiphenyl.

^{1}H NMR ($CDCl_3$, 400.13 MHz): δ 7.62–7.52 (m, 4H), 7.50–7.40 (m, 4H), 7.36–7.30 (m, 1H), 1.37 (s, 9H).

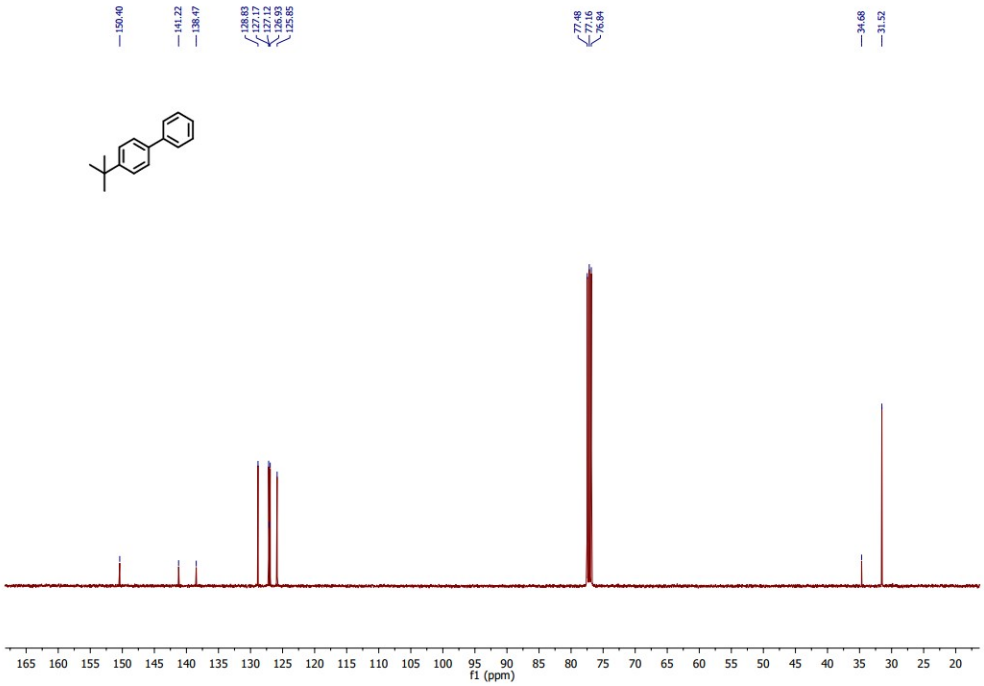

Figure S24. ^{13}C NMR ($CDCl_3$) spectrum of 4-*tert*-butylbiphenyl.

$^{13}C\{^{1}H\}$ NMR ($CDCl_3$, 100.61 MHz): δ 150.4, 141.2, 138.5, 128.8, 127.2, 127.1, 126.9, 125.9, 34.7, 31.5.

^{1}H and ^{13}C NMR data in agreement with the literature.[2]

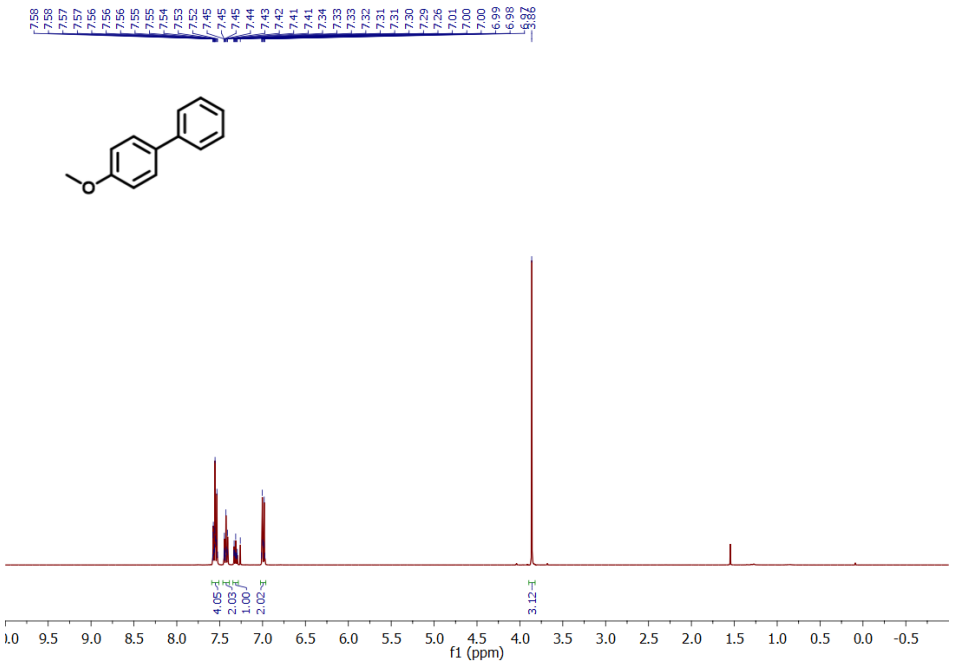

Figure S25. ^{1}H NMR ($CDCl_3$) spectrum of 4-methoxybiphenyl.

^{1}H NMR ($CDCl_3$, 400.13 MHz): δ 7.59–7.51 (m, 4H), 7.46–7.39 (m, 2H), 7.35–7.28 (m, 1H), 7.02–6.96 (m, 2H), 3.86 (s, 3H).

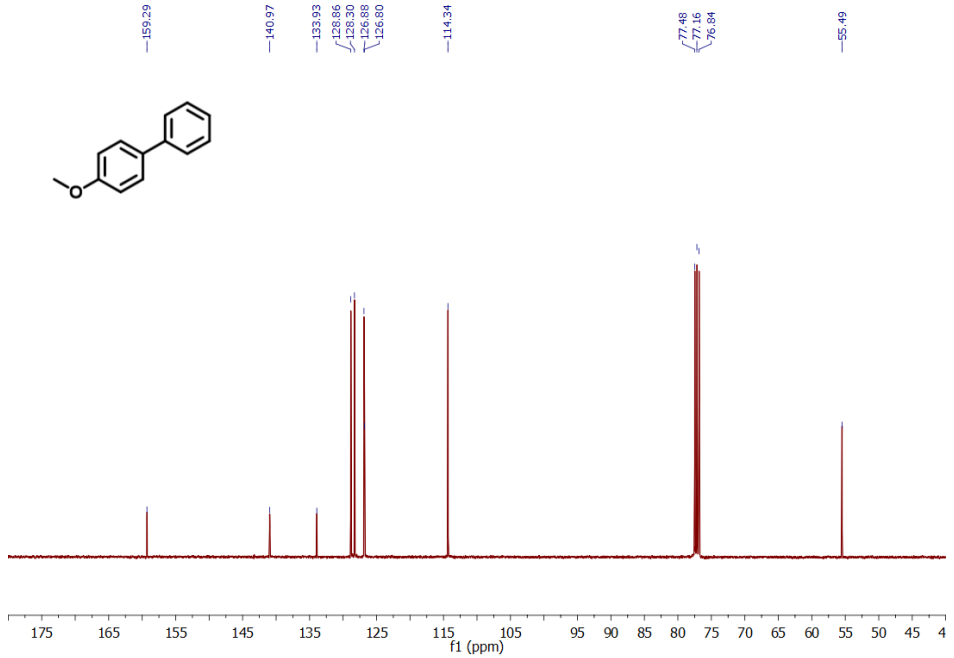

Figure S26. ^{13}C NMR ($CDCl_3$) spectrum of 4-methoxybiphenyl.

$^{13}C\{^{1}H\}$ NMR ($CDCl_3$, 100.61 MHz): δ 159.3, 141.0, 133.9, 128.9, 128.3, 126.9, 126.8, 114.3, 55.5.

^{1}H and ^{13}C NMR data in agreement with the literature.[3,4]

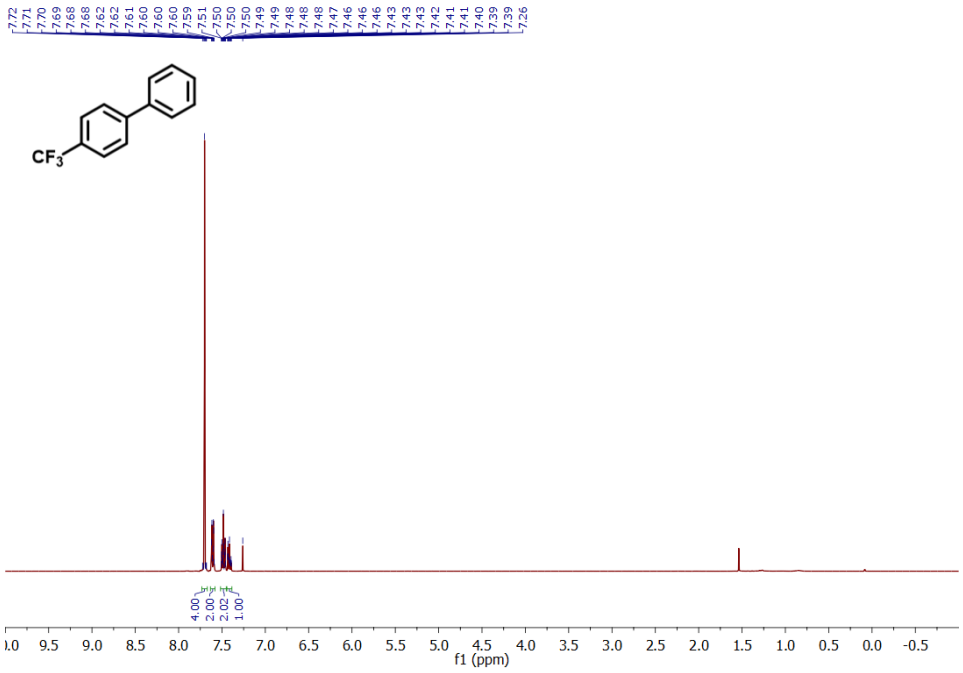

Figure S27. ^{1}H NMR ($CDCl_3$) spectrum of 4-trifluoromethylbiphenyl.

^{1}H NMR ($CDCl_3$, 400.13 MHz): δ 7.70 (m, 4H), 7.63–7.58 (m, 2H), 7.52–7.45 (m, 2H), 7.44–7.39 (m, 1H).

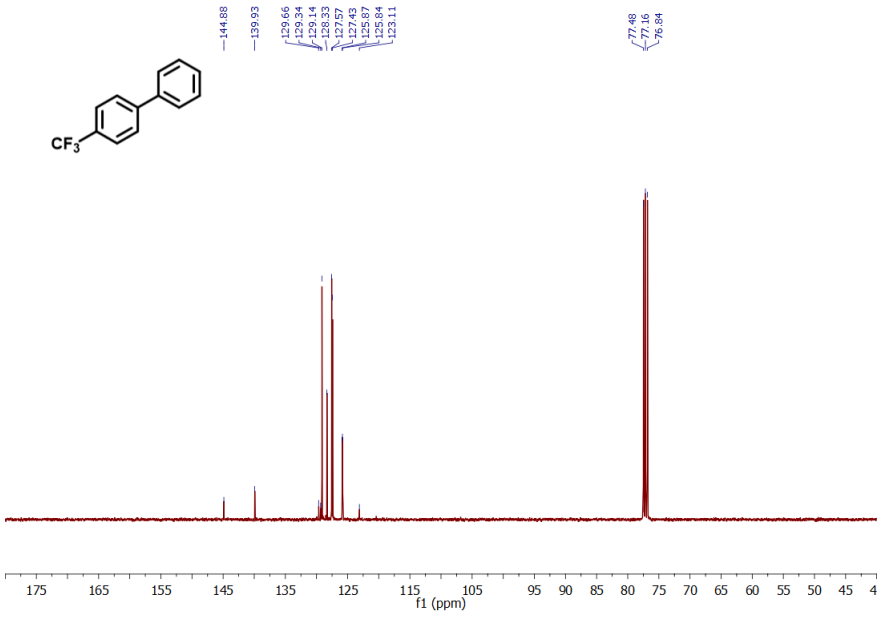

Figure S28. ^{13}C NMR ($CDCl_3$) spectrum of 4-trifluoromethylbiphenyl.

^{13}C{^{1}H} NMR ($CDCl_3$, 100.61 MHz): δ 144.9, 139.9, 129.4 (q, ^{2}J = 32.4 Hz), 129.1, 128.3, 127.6, 127.4, 125.9 (q, ^{3}J = 3.7 Hz), 124.5 (q, ^{1}J = 272.0 Hz).

^{1}H and ^{13}C NMR data in agreement with the literature.[5]

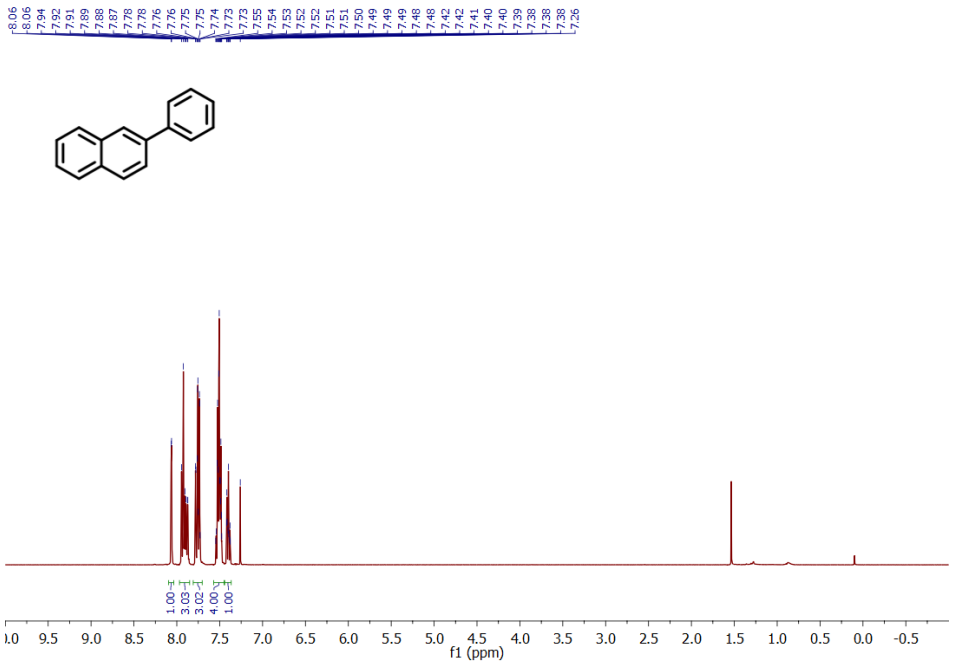

Figure S29. ^{1}H NMR ($CDCl_3$) spectrum of 2-phenylnaphthalene.

^{1}H NMR ($CDCl_3$, 400.13 MHz): δ 8.06 (d, J = 1.8 Hz, 1H), 7.97–7.85 (m, 3H), 7.81–7.70 (m, 3H), 7.57–7.45 (m, 4H), 7.44–7.37 (m, 1H).

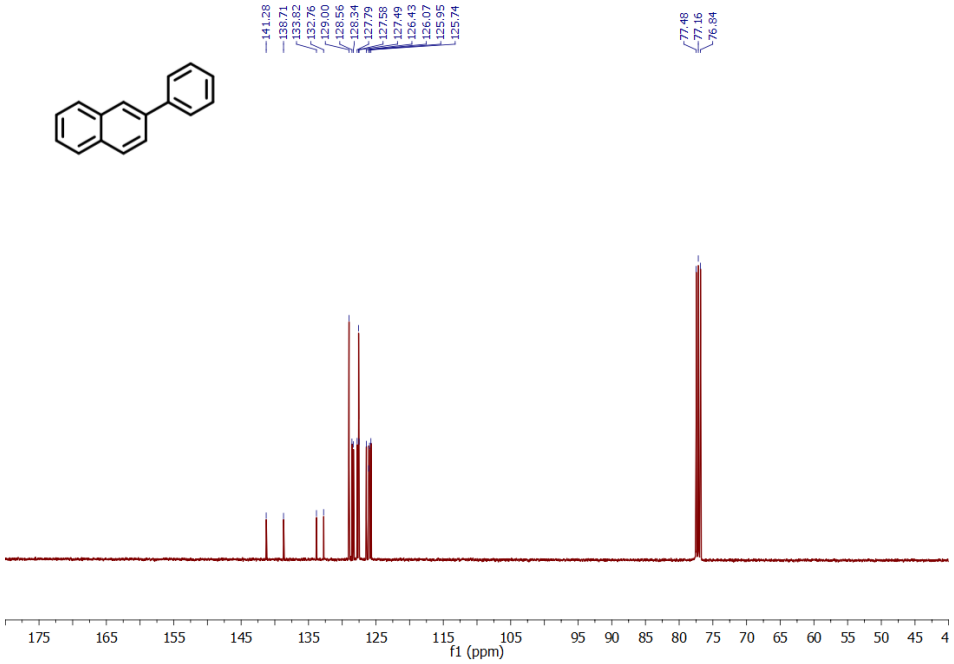

Figure S30. ^{13}C NMR ($CDCl_3$) spectrum of 2-phenylnaphthalene.

$^{13}C\{^{1}H\}$ NMR ($CDCl_3$, 100.61 MHz): δ 141.3, 138.7, 133.8, 132.8, 129.0, 128.6, 128.3, 127.8, 127.6, 127.5, 126.4, 126.1, 126.0, 125.7.

^{1}H and ^{13}C NMR data in agreement with the literature.[3,4]

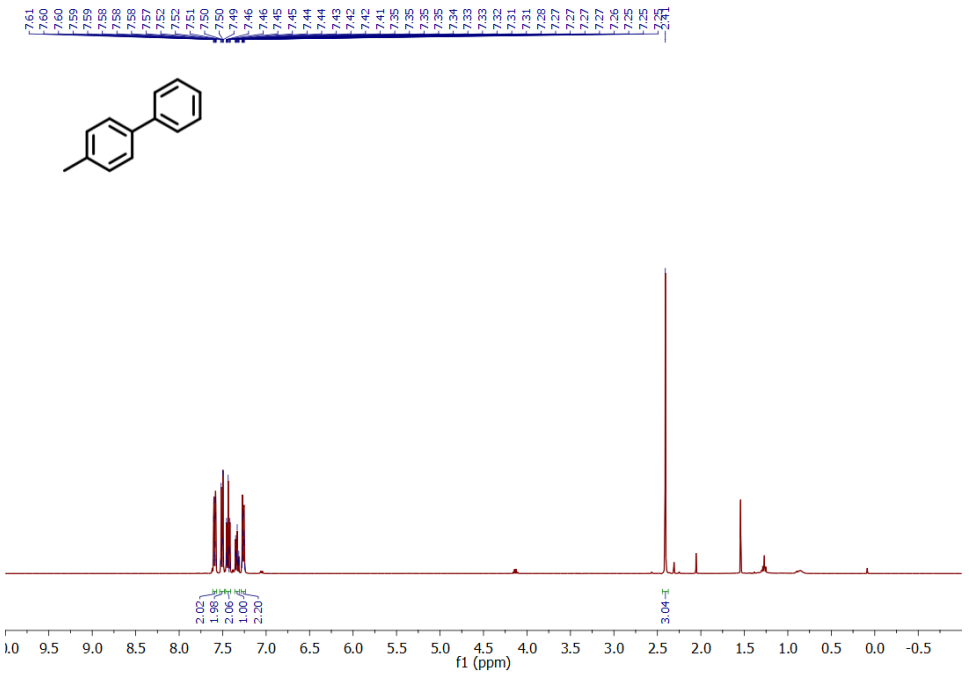

Figure S31. ^{1}H NMR ($CDCl_3$) spectrum of 4-methyl-1,1'-biphenyl.

^{1}H NMR ($CDCl_3$, 400.13 MHz): δ 7.61–7.57 (m, 2H), 7.53–7.48 (m, 2H), 7.47–7.41 (m, 2H), 7.36–7.31 (m, 1H), 7.29–7.24 (m, 2H), 2.41 (s, 3H).

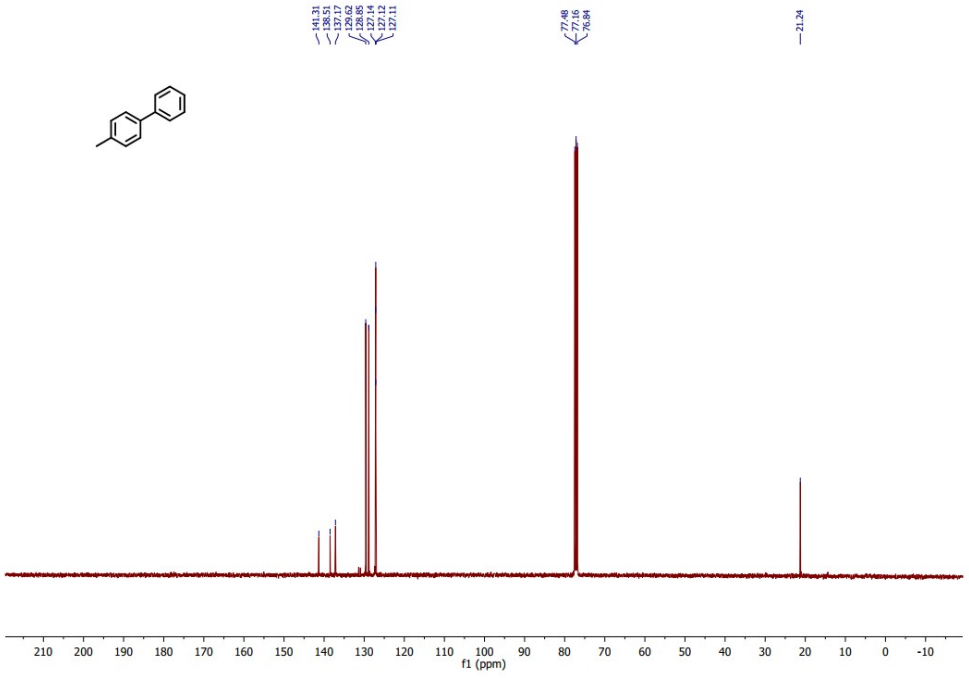

Figure S32. ^{13}C NMR ($CDCl_3$) spectrum of 4-methyl-1,1'-biphenyl.

^{13}C{^{1}H} NMR ($CDCl_3$, 100.61 MHz): δ 141.3, 138.5, 137.2, 129.6, 128.9, 127.1, 127.1, 127.1, 21.2.

^{1}H and ^{13}C NMR data in agreement with the literature.[3,4]

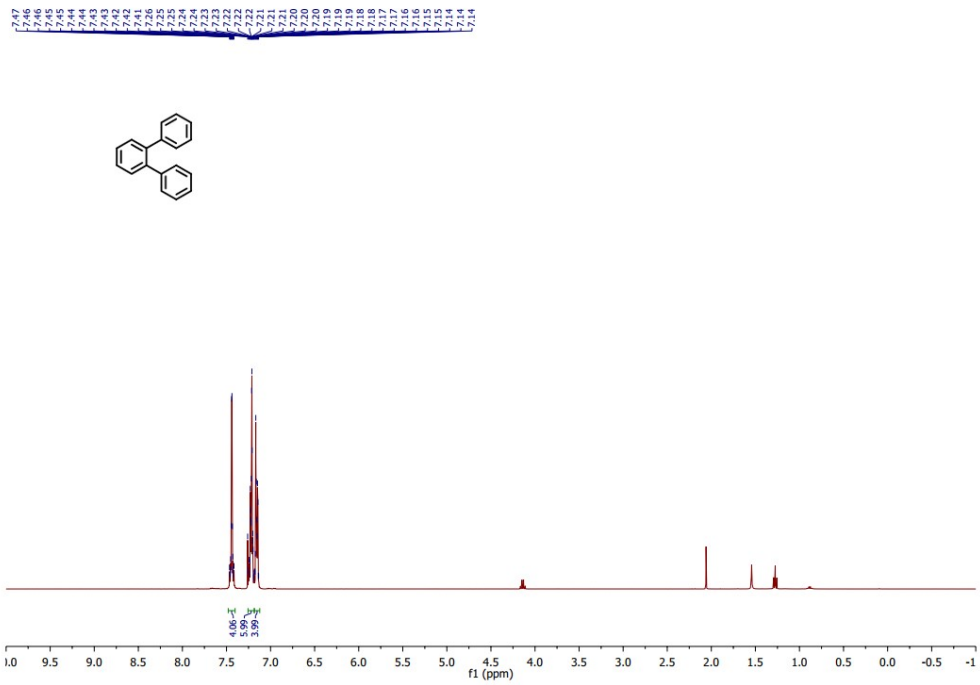

Figure S33. ^{1}H NMR ($CDCl_3$) spectrum of *o*-terphenyl.

^{1}H NMR ($CDCl_3$, 400.13 MHz): δ 7.47–7.41 (m, 4H), 7.26–7.18 (m, 6H), 7.18–7.12 (m, 4H).

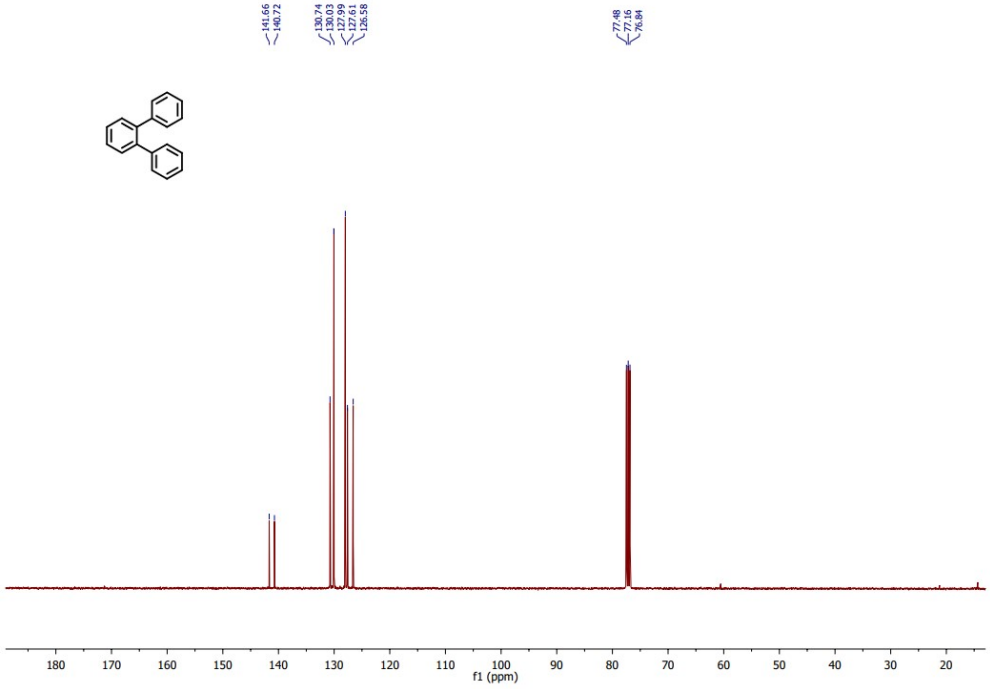

Figure S34. ^{13}C NMR ($CDCl_3$) spectrum of *o*-terphenyl.

$^{13}C\{^{1}H\}$ NMR ($CDCl_3$, 100.61 MHz): δ 141.7, 140.7, 130.7, 130.0, 128.0, 127.6, 126.6.

^{1}H and ^{13}C NMR data in agreement with the literature.[6]

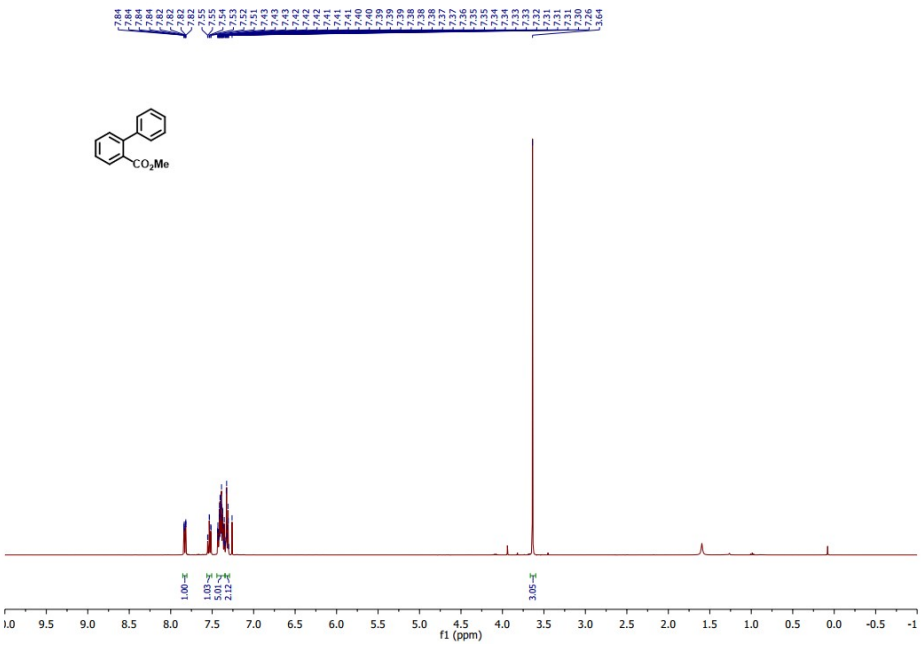

Figure S35. ^{1}H NMR ($CDCl_3$) spectrum of methyl 2-phenylbenzoate.

^{1}H NMR ($CDCl_3$, 400.13 MHz): δ 7.83 (ddd, J = 7.6, 1.4, 0.5 Hz, 1H), 7.53 (td, J = 7.5, 1.4 Hz, 1H), 7.44–7.35 (m, 5H), 7.34–7.29 (m, 2H), 3.64 (s, 3H).

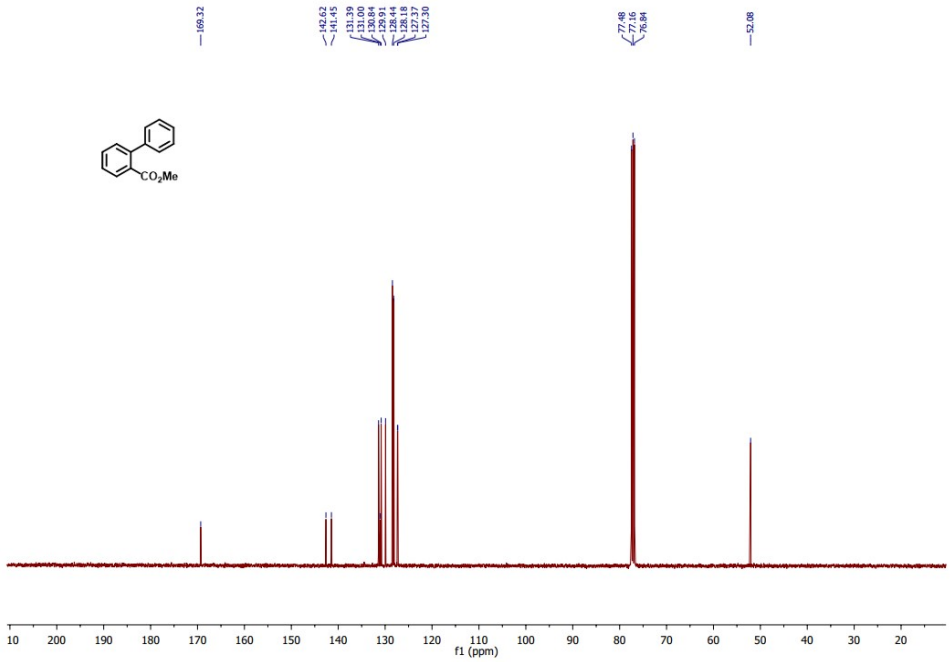

Figure S36. ^{13}C NMR ($CDCl_3$) spectrum of methyl 2-phenylbenzoate.

$^{13}C\{^{1}H\}$ NMR ($CDCl_3$, 100.61 MHz): δ 169.3, 142.6, 141.5, 131.4, 131.0, 130.8, 129.9, 128.4, 128.2, 127.4, 127.3, 52.1.

^{1}H and ^{13}C NMR data in agreement with the literature.[7]

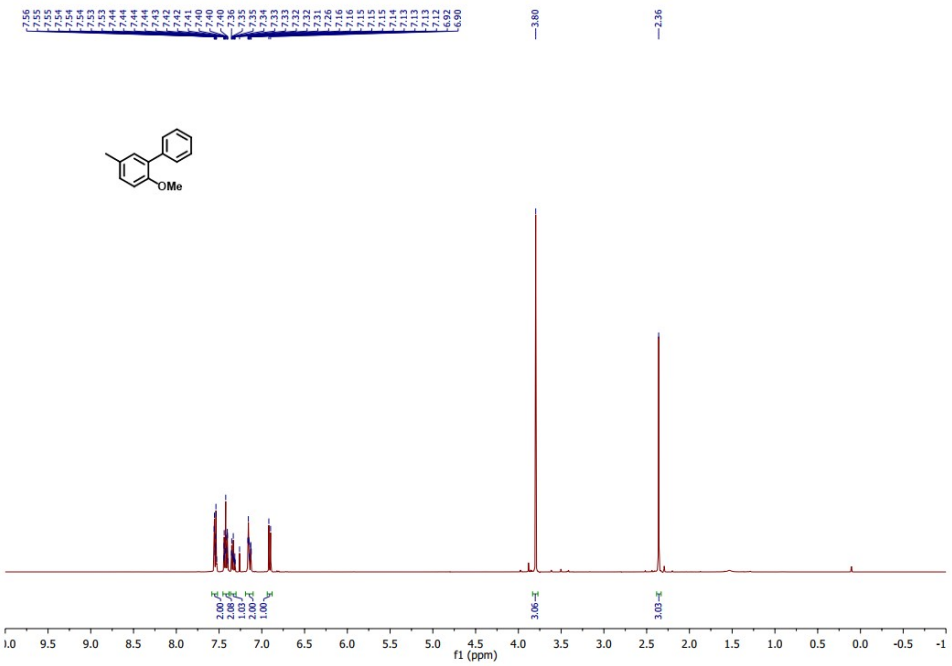

Figure S37. ^{1}H NMR ($CDCl_3$) spectrum of 2-methoxy-5-methyl-1,1'-biphenyl.

^{1}H NMR ($CDCl_3$, 400.13 MHz): δ 7.58–7.52 (m, 2H), 7.45–7.38 (m, 2H), 7.37–7.30 (m, 1H), 7.19–7.10 (m, 2H), 6.91 (d, J = 8.2 Hz, 1H), 3.80 (s, 3H), 2.36 (s, 3H).

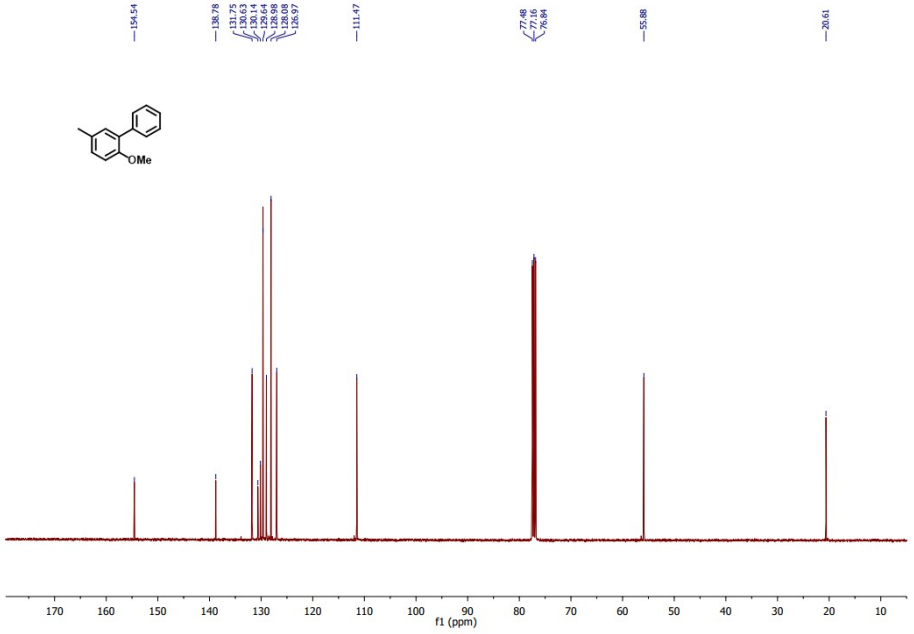

Figure S38. ^{13}C NMR ($CDCl_3$) spectrum of 2-methoxy-5-methyl-1,1'-biphenyl.

^{13}C{^{1}H} NMR ($CDCl_3$, 100.61 MHz): δ 154.5, 138.8, 131.8, 130.6, 130.1, 129.6, 129.0, 128.1, 127.0, 111.5, 55.9, 20.6.

^{1}H and ^{13}C NMR data in agreement with the literature.[8]

References

1. H. Zeng, D. Cao, Z. Qiu and C.-J. Li, *Angew. Chem. Int. Ed*., 2018, **57**, 3752–3757.
2. J. P. Wolfe, R. A. Singer, B. H. Yang and S. L. Buchwald, *J. Am. Chem. Soc.*, 1999, **121**, 9550–9561.
3. W. Liu, H. Cao, H. Zhang, H. Zhang, K. H. Chung, C. He, H. Wang, F. Y. Kwong and A. Lei, *J. Am. Chem. Soc.*, 2010, **132**, 16737–16740.
4. S.-Y. Ding, J. Gao, Q. Wang, Y. Zhang, W.-G. Song, C.-Y. Su and W. Wang, *J. Am. Chem. Soc.*, 2011, **133**, 19816–19822.
5. E. J. Cho, T. D. Senecal, T. Kinzel, Y. Zhang, D. A. Watson and S. L. Buchwald, *Science*, 2010, **328**, 1679–1681.
6. G. Liu, F. Han, C. Liu, H. Wu, Y. Zeng, R. Zhu, X. Yu, S. Rao, G. Huang, J. Wang, *Organometallics*, 2019, **38**, 1459–1467.
7. S. Santra, P. K. Hota, R. Bhattacharyya, P. Bera, P. Ghosh, S. K. Mandal, *ACS Catal.*, 2013, **3**, 2776–2789.
8. X. Xiong, R. Zhu, L. Huang, S. Chang, J. Huang, *Synlett*, 2017, **28**, 2046–2050.